Author/s:
Chou, ES;Abidi, SZ;Teye, M;Leliwa-Sytek, A;Rask, TS;Cobbold, SA;Tonkin-Hill, GQ;Subramaniam, KS;Sexton, AE;Creek, DJ;Daily, JP;Duffy, MF;Day, KP

Title:
A high parasite density environment induces transcriptional changes and cell death in Plasmodium falciparum blood stages

Date:
2018-03-01

Citation:
Chou, E. S., Abidi, S. Z., Teye, M., Leliwa-Sytek, A., Rask, T. S., Cobbold, S. A., Tonkin-Hill, G. Q., Subramaniam, K. S., Sexton, A. E., Creek, D. J., Daily, J. P., Duffy, M. F. & Day, K. P. (2018). A high parasite density environment induces transcriptional changes and cell death in Plasmodium falciparum blood stages. FEBS Journal, 285 (5), pp.848-870. https://doi.org/10.1111/febs.14370.

Article type : Regular Paper

Color : Figs 1-9

SuppInfo : 11 Tables

Title: A High Parasite Density Environment Induces Transcriptional Changes and Cell Death in *Plasmodium falciparum* Blood Stages

Running title: High Density Induces *P. falciparum* Cell Death

Authors: Evelyn S. Chou[1]†, Sabia Z. Abidi[2]†, Marian Teye[3], Aleksandra Leliwa-Sytek[3], Thomas S. Rask[3], Simon A. Cobbold[1], Gerry Q. Tonkin-Hill[4], Krishanthi S. Subramaniam[5], Anna E. Sexton[6], Darren J. Creek[6], Johanna P. Daily[7], Michael F. Duffy[1], Karen P. Day[1*]

Affiliations:

[1]Bio21 Institute for Molecular Science and Biotechnology and School of BioSciences, University of Melbourne, Parkville, Victoria 3052, Australia

[2]Department of Materials Science and Engineering, Massachusetts Institute of Technology, Cambridge, MA 02139 USA

[3]Department of Microbiology, Division of Medical Parasitology, New York University School of Medicine, New York, NY 10010 USA

[4]Walter and Eliza Hall Institute of Medical Research, Parkville, Victoria 3052, Australia

[5]Department of Parasitology, Liverpool School of Tropical Medicine, Pembroke Place, Liverpool L3 5QA, United Kingdom

[6]Drug Delivery Disposition and Dynamics, Monash Institute of Pharmaceutical Sciences, Monash University, Parkville, Victoria 3052, Australia

[7]Department of Medicine, Department of Microbiology & Immunology, Albert Einstein College of Medicine, Bronx, NY 10461 USA

†These authors contributed equally to this work.

*Correspondence to:

Professor Karen P. Day

Dean, Faculty of Science

Address: Ground Floor, Old Geology Building

University of Melbourne

Victoria 3010

Email: Karen.Day@unimelb.edu.au

Phone: +61 3 8344 6407

Abbreviations: HD: high density; LD: low density; U: uninfected erythrocytes; CM: conditioned medium; MMP: mitochondrial membrane potential; Pf: *Plasmodium falciparum*

Database: gene expression data are available in the GEO databases under the accession number **GSE91188**.

Keywords: *Plasmodium falciparum*; microarray; transcription; density; stress response**Abstract**

Transient regulation of *Plasmodium* numbers below the density that induces fever has been observed in chronic malaria infections in humans. This species transcending control cannot be

explained by immunity alone. Using an *in vitro* system we have observed density dependent regulation of malaria population size as a mechanism to possibly explain these *in vivo* observations. Specifically, *P. falciparum* blood stages from a high but not low-density environment exhibited unique phenotypic changes during the late trophozoite and schizont stages of the intraerythrocytic cycle. These included in order of appearance: failure of schizonts to mature and merozoites to replicate, apoptotic-like morphological changes including shrinking, loss of mitochondrial membrane potential, and blebbing with eventual release of aberrant parasites from infected erythrocytes. This unique death phenotype was triggered in a stage-specific manner by sensing of a high-density culture environment. Conditions of glucose starvation, nutrient depletion, and high lactate could not induce the phenotype. A high-density culture environment induced rapid global changes in the parasite transcriptome including differential expression of genes involved in cell remodeling, clonal antigenic variation, metabolism, and cell death pathways including an apoptosis-associated metacaspase gene. This transcriptional profile was also characterized by concomitant expression of asexual and sexual stage-specific genes. The data show strong evidence to support our hypothesis that density sensing exists in *P. falciparum.* They indicate that an apoptotic-like mechanism may play a role in *P. falciparum* density regulation, which, as in yeast, has features quite distinguishable from mammalian apoptosis.

Introduction

Protozoan parasites of genus *Plasmodium* are responsible for human malaria, a vector-borne febrile illness that impacts nearly half of the world's population. Chronic *Plasmodium* infections have been associated with regulation of within-host parasite numbers that could not be explained by innate or acquired immunity alone, suggesting that maintenance of population size may also be a behavioral response by the parasite to conditions of high parasite density [1–3]. Such regulated responses are commonly utilized in microorganisms to maximize community longevity, following exposure to various antagonists including drug pressure, immunity, resource scarcity, and inter-species or inter-genotype competition. In such cases, regulation or reduction of microbial population density via cell fate decision-making or programmed cell death can increase the overall fitness of the community.

In prokaryotic microorganisms, density sensing via the production and recognition of autoinducers is integral to the regulation of biofilm formation, adhesion, and expression of virulence factors in response to environmental change [4]. The opportunistic pathogen *Pseudomonas aeruginosa* produces an acyl-homoserine lactone that activates expression of two density-sensing circuits, resulting in an upregulation of genes encoding toxins and extracellular enzymes [5]. Density sensing is also a feature of eukaryotic unicellular organisms. For example, yeast populations respond to environmental changes by producing toxins, pheromones, and other secreted molecules [6–8]. In the polymorphic fungus *C. albicans*, transitions between budding yeast growth, filamentous growth, and apoptotic cell death are determined by the delicate interplay of two secreted molecules tyrosol and farnesol [8–10]. While elevated levels of tyrosol result in an upregulation of cell cycle regulation and DNA repair pathways, farnesol depletes cellular antioxidants by conjugating with intracellular glutathione, allowing Cdr1p-mediated extrusion of the glutathione conjugate and inducing apoptosis [11].

Evidence of density and environmental sensing has also been observed in protozoan parasites. For example, differentiation from the slender to stumpy forms in *Trypanosoma brucei brucei* is induced by the density-dependent "stumpy-initiating factor" (SIF) through a putative mechanism involving cAMP-dependent signaling and the RNA-binding protein RBP7 [12–14]. Differentiation of asexual *Plasmodium falciparum* to the transmissible gametocyte form is similarly density-dependent and can be induced by soluble factors [15–20]. Furthermore, earlier studies have reported an array of controlled responses to environmental changes in *Plasmodium* spp., including programmed cell death and coordinated transcriptional modification after exposure to extreme conditions such as febrile temperatures, nutrient depletion and antimalarial drug treatment [21–24].

Here we explore whether density or environmental sensing occurs in *P. falciparum* in a manner analogous to yeast environmental response mechanisms. Parasites were cultured *in vitro* to study the parasite response to density in the absence of host immune factors, testing the hypothesis that parasites may regulate their own population as posited by Bruce and colleagues [25]. An isolated system provided a means to study inter-parasite communication without the confounding

influences of external regulatory forces. *In vitro* studies of density sensing are commonly used for other microorganisms, as in the fungi *Candida albicans* and *Cryptococcus neoformans* [8–10,26]. Using the *in vitro* culture system, we examined the effect of high parasite density on *P. falciparum* asexual viability and replication, and the role of nutrient sensing in cultures with high density and high metabolic activity. Comparison of asexual blood stage development under low and high-density conditions revealed a unique, density-dependent death phenotype with hallmarks of yeast apoptosis. Transcriptional profiling showed putative early responses to high density typified by upregulation of pathways involved in cell death and clonal antigenic variation, as well as dysregulation of sexual stage gene expression.

Results

High-density cultures inhibit parasite development at trophozoite stage

The 3D7 *P. falciparum* clone from the Walliker Cross was maintained *in vitro* under conditions of limited passage and was frequently subcultured such that parasite density never exceeded $2x10^4$ parasites per microliter of culture (see methods). Parasites were then cultured without dilution for 3 full cycles over 6 days, with daily medium changes. After 4 days, parasite density had exceeded $3x10^4$ parasites per microliter and a reduction in parasite population size was subsequently observed (**Fig. 1A**). Mature schizonts and reinvading rings were not observed after reaching this density threshold, but rather a high proportion of aberrant parasites that were released from the erythrocytes **(Fig. 1B)**.

A 2-day culture assay was developed to investigate whether the reduction in population size at high density was due to a failure of 1) schizont maturation/merogony, 2) egress, or 3) ring reinvasion. Parasites were synchronized in order to isolate stage-specific effects while approximating the *in vivo* conditions experienced by parasites during an infection. Synchronicity of infection has been observed in the bloodstream as characterized by periodicity of multiplication over a 48-hour cycle, as well as in the capillaries where mature stages sequester [27,28]. In contrast, *in vitro* parasite cultures revert to asynchronicity, resulting in mixed cultures comprising all stages of parasite development [29–32]. Various studies have shown that parasite gene expression and metabolism are temporally hardwired, such that a mixed parasite culture would confound results due to conflicting rates of transcription, metabolic activity, protein

production and other biological functions [33,34]. Therefore, a synchronous culture was necessary to fully understand the effects of density on parasite behavior. This system was used to measure the effects of parasite density on stage-specific development during the trophozoite and early schizont stages (18-36hpi and 36-42hpi, respectively). Two extreme conditions were chosen to examine the response to parasite density where high-density cultures (HD; greater than $3x10^4$ parasites per microliter of culture) and low-density cultures (LD; less than $5x10^3$ parasites per microliter of culture) were fed with fresh complete culture media at 18hpi and observed over the 30-hour period of trophozoite and schizont development (**Fig. 2A**). Population size in the HD culture was drastically reduced due to failure of schizont maturation and merozoite formation, whereas the LD culture exhibited normal parasite development throughout ring, trophozoite, and schizont stages, followed by reinvasion as rings (**Fig. 2B, Fig. 2C, Fig. 3**). Differences in differential counts between HD and LD cultures were statistically significant for all parasite stages at both 40hpi and 50hpi (one-way ANOVA with Tukey's post-hoc test; both $p < 0.05$). Trophozoite populations at 30hpi were not significantly altered in HD culture relative to LD culture ($p > 0.05$).

The majority of parasites in HD culture failed to develop beyond the early schizont stage **(Fig. 2B, Fig. 2C, Fig. 3).** An imaging time course revealed the appearance of aberrant parasites by 40hpi, characterized by a shrunken, irregular shape, amoeboid projections extending from the parasite cell membrane, and dense, compacted pigment when stained with Giemsa, indicating the completion of hemoglobin digestion and hemozoin formation. Autophagy-associated vacuole formation was never observed in the aberrant parasites. At 45hpi, a significant proportion of aberrant parasites, resembling younger trophozoites in size, were released from erythrocytes in high-density cultures only (45hpi, 10±2%; 50hpi, 30±7%; one-way ANOVA, $p < 0.0001$) **(Fig. 2B).** Similarly sized parasites have been seen previously *in vivo* in the spleen [35]. Release of aberrant parasites in HD cultures coincided with time of merozoite release in LD cultures. The sequence of morphological changes in a high-density parasite culture, defined here as the "density-dependent death phenotype", includes (1) failure of early schizont maturation at 35hpi; (2) failure of merogony by 40hpi; and (3) cell shrinking and blebbing and (4) release of intact parasites from erythrocytes from 40 to 50hpi (**Fig. 2B)**.

To assess the degree of cell shrinking throughout high-density, late stage parasite maturation, parasitized erythrocytes were stained with a BODIPY-TR-ceramide lipid dye for two hours prior to fixation and imaged in optical sections to generate a 3D reconstruction of the parasite membrane. Volumetric measurements of parasites grown at high or low density at four time points between 30 and 50hpi demonstrated inhibition of parasite cell growth initiated during early schizont stage in high-density cultures of parasites. In contrast, parasites grown at low density exhibited a continual increase in size that peaked around late schizont stage (HD vs. LD: one-way ANOVA with Tukey's post-hoc test; $p < 0.01$ for time points 36, 45, 50hpi) (**Fig. 2D, Fig. 3).**

To test whether high-density cultures shared similarities with yeast programmed cell death, we measured the loss of mitochondrial membrane potential (MMP) in high and low-density parasite cultures (**Fig. 2E**) [36]. MMP was measured as the percentage of parasites negative by flow cytometry for the dye JC-1. Density-dependent death was morphologically visible by 45hpi in high-density cultures, but the proportion of JC-1-negative high-density parasites at 45hpi was not significantly different compared to earlier time points. At 50hpi, 100% of high-density parasites exhibited density-dependent death morphology and 70±3% were JC-1 negative, a significant increase compared to earlier time points (two-way ANOVA with Tukey's post-hoc test; $p < 1e10^{-7}$). Post-hoc testing for interaction effects further revealed that JC-1 negativity was significantly different between high and low density cultures, particularly at 50hpi (LD-HD: $p < 1e10^{-7}$; LD50-HD50: $p < 1e10^{-7}$). DNA fragmentation throughout parasite maturation as measured by TUNEL staining was not significantly different between high and low-density cultures (two-way ANOVA; $p > 0.1$). Aberrant parasite morphology was not observed in LD cultures during development (**Fig. 2E**).

Cytoadherence is not affected in parasites cultured at high density

P. falciparum sequesters at high density in lung, heart and adipose tissue at trophozoite stage. To investigate the effect of density-dependent death on the ability of *P. falciparum* to sequester, we performed cytoadherence assays using C32 melanoma cells with infected erythrocytes cultured at low and high parasite density. Cytoadherence assays were performed using 40-42hpi parasites at which point the high-density death phenotype was already apparent. High and low-density

infected erythrocytes adhered at concentrations of 157±19 and 117±22 per 100 C32 melanoma cells (mean±sd). No significant reduction in cytoadherence in high-density parasites was observed.

High-density conditioned medium operates in parasite density ranges relevant to human malaria

To determine whether density-dependent death of *P. falciparum* mature blood stages could be induced by parasite-released factors present in the surrounding media, conditioned medium (CM) from parasite culture was added to logarithmically growing, low-density late trophozoites (**Fig. 4A**). The CM was harvested from highly synchronous late trophozoite to early schizont stage parasite populations ranging between 10^2 – 10^5 parasites per microliter, and thus contained late-stage parasite metabolites and other secreted factors from cultures grown at densities consistent with the densities observed in semi-immune, asymptomatic children (below 1000 parasites per microliter of blood) [25]. Low-density trophozoites incubated in CM were assessed for morphological aberration after a period of 12 hours, when parasites would normally appear as early schizonts. Density-dependent death was identified using Giemsa smears to determine whether parasite morphology aligned with the characteristic features observed in **Figure 2B**. Incubation in CM harvested from trophozoite populations in the range of 10^2 to 10^4 parasites per microliter resulted in partial inhibition of parasite growth. However, CM harvested from parasite densities of 10^5 parasites per microliter induced the density-dependent death phenotype in 100% of parasites, a significant increase from parasites incubated in CM from lower parasite densities (one-way-ANOVA with Tukey's post-hoc test; $p < 0.001$) (**Fig. 4A**).

CM was harvested from mature stages incubated at high and low density for 18 hours and used for additional testing on late-stage, low-density trophozoites (**Fig. 4B**). As in **Figure 4A**, high-density conditioned medium (HDCM; harvested from parasite cultures greater than $3x10^4$ parasites per microliter) consistently produced density-dependent cell death when incubated on logarithmically growing, low-density late trophozoites. These dying cells were identical to cells dying from growth at high density and exhibited the same phenotypes of failure of schizont maturation and merogony, cell shrinking, membrane blebbing and release from erythrocytes. Aberrations in parasite development and viability were not observed when incubated in low-

density conditioned medium (LDCM; harvested from parasite cultures less than $5x10^3$ parasites per microliter) (**Fig. 4C**). CM harvested from ruptured low-density schizonts resulting in high densities of early rings (ER, 0-8hpi), or from high-density cultures of late ring or early trophozoite stages (LR, 8-16hpi; ET, 18-30hpi) also failed to induce the death phenotype in test cultures (**Fig. 4D**). HDCM-induced cell death and aberrant morphology were diminished following titration below a threshold concentration of 80%, whereas concentrations of 80% or greater were sufficient to generate the density-dependent death phenotype in at least 50% of trophozoites in low-density culture (**Fig. 4E**) suggesting that the death phenotype is triggered by HDCM in a concentration-dependent manner. CMs harvested from multiple strains induced failure of merogony and cell death in both homologous and heterologous parasite isolates and clones, indicating that the observed killing activity is not strain-specific (**Fig. 4F**).

Nutrient supplementation delays but does not prevent the high-density death phenotype

Glucose starvation and lactic acid accumulation can detrimentally affect parasite growth during the asexual stages *in vitro* [37,38] and the levels of these nutrients would likely be altered in HDCM. Normal glucose concentrations in human sera range between 3.89mM and 7.22mM, while lactic acid concentrations above 16mM and glucose levels below 4mM are reported to have inhibitory effects on *P. falciparum* growth rate [22,37]. To understand the rate of glucose depletion throughout the duration of an HD culture experiment (18-42hpi) and its possible role in the observed phenotype, we measured the glucose concentration in HD and LD cultures. A time course of CM samples was collected from HD, LD and uninfected erythrocyte cultures at 6-hour intervals from 18hpi to 48hpi. Glucose and lactate concentrations at each time point were measured using gas chromatography mass spectrometry (GC-MS). Glucose concentration decreased dramatically in HD culture between 24-42hpi (~11mM to ~1mM) (**Fig. 5, left panel**) to levels that would be described as hypoglycemic *in vivo* (below 4mM). This was expected due to the high glycolytic activity associated with this part of the life cycle [38]. Glucose levels in LD cultures, in contrast, decreased only marginally throughout the duration of culture (~11mM to 8.2mM). Lactic acid levels in HD cultures exceeded 16mM after 36hpi or 18 hours in culture, but this threshold was never exceeded in LD cultures even after 30 hours in culture (**Fig. 5, right panel)**. Glucose and lactic acid metabolism was also measured for uninfected erythrocytes at culture conditions (5% hematocrit) and *in vivo* conditions (40% hematocrit). While uninfected

erythrocytes at 5% hematocrit metabolized glucose and lactic acid at a minimal rate, never exceeding toxic thresholds even after a 30-hour incubation, metabolism at 40% hematocrit reached growth-limiting levels between 12 and 18 hours. In contrast to glucose and lactate, essential amino acids and vitamins [39,40] were not significantly depleted in HDCM but were present at comparable levels to LDCM and UCM controls **(Table S1)**.

Supplementation assays were performed to determine the role of glucose depletion or lactate toxicity in density-dependent cell death. Decreasing glucose below the hypoglycemic threshold of 4mM for 24 hours resulted in a sharp decline in the numbers of ring stages in the following cycle, and high-density parasite cultures replenished with glucose exhibited a lesser degree of cell shrinking at the nominal schizont stage compared to those without supplementation, suggesting that glucose starvation plays a role in cell shrinking (**Fig. 6A, Fig. 6B**). However, supplementing HDCM with glucose to the levels found in fresh media or higher (up to 20mM) neither rescued parasite viability to control levels nor prevented aberrant growth, and therefore glucose depletion cannot have caused the HDCM-induced, density-dependent death phenotype (**Fig. 6C).** Linear modelling of HDCM and glucose-depleted media titrations revealed that dynamic responses to density and glucose starvation are significantly different, highlighting a clear distinction between the density-dependent death phenotype and cell death due to starvation (ANOVA, $p = 1.4e^{-9}$). Normal growth, characterized by replication rate consistent with parasites incubated in control complete culture medium and absence of aberrant schizont morphology, was observed in LDCM-treated samples regardless of glucose supplementation. Lactate supplementation up to 40mM in LDCM also failed to reduce parasite replication rate or induce density-dependent death (**Fig. 6C**).

Replenishing the culture medium at multiple time points throughout trophozoite development did not rescue high-density parasites from undergoing the density-dependent death phenotype prior to schizont maturation (**Fig. 6D**). However, reducing parasite density by subculture from $3x10^4$ parasites per microliter to $5x10^3$ parasites per microliter at late trophozoite stage prevented density-dependent death and allowed progression to ring stage. This finding strongly suggests that high parasite density rather than nutrient depletion *per se* induces the death phenotype in the majority of the parasite population.

Removal of microvesicles does not prevent density-dependent killing

Recent publications have suggested that cellular communication in *Plasmodium* takes place via transport of intracellular material within microvesicles and exosome-like vesicles [20,41]. To explore the potential role of microvesicles in the induction of the high-density death phenotype, 100nm fractions were removed from HDCM using filtration units and trophozoites were incubated with the filtrate for 12 hours. There was no difference in density-dependent death between parasites treated with filtered HDCM (78%) and parasites treated with unfiltered HDCM (85%) (Student's t-test; $p > 0.05$), proving that the density dependent death phenotype was due to soluble factors and not microvesicles.

Transcriptome analysis

Transcriptional profiling was performed to explore the effect of a high-density environment on *P. falciparum* gene expression compared to a low-density environment. Fresh complete culture medium was added to high-density and low-density parasite cultures at 18hpi, incubated for 18 hours, and then harvested at 36hpi to collect the conditioned medium (CM). Low-density, late-stage trophozoites were then incubated for 2 hours with the CM harvested from uninfected erythrocytes (U), low-density (LD) or high-density (HD) parasites before RNA extraction for microarray analysis. This relatively short incubation period was chosen to ensure maximal parasite viability and RNA integrity at time of RNA harvest as well as synchronicity, parameters difficult to obtain in high-density cultures after longer exposure to high-density environments. To evaluate the effects of CM treatment on transcriptional activity, late stage trophozoites were chosen because of the high metabolic activity and morphological changes previously observed in these stages, both in the literature and in the high-density culture system [34,42].

A two-hour incubation in HDCM did not significantly affect parasite morphology, replication rate or mitochondrial membrane potential (data not shown). However, parasites underwent significant changes after 12 hours, as described earlier (**Fig. 4C, Fig. 4D**). In contrast, parasites

were not developmentally affected by incubations with LDCM or UCM for up to 18 hours (**Fig. 4C, Fig. 6C**). Gametocytes were not observed in any of the conditions throughout the duration of the experiment, nor were any significant differences in mean gametocyte production found in a 7-day culture assay following two-hour incubation in HDCM, LDCM, or UCM (one-way ANOVA; $p > 0.1$).

Global differences in gene expression were observed after the two-hour incubation in CM when comparing between parasites incubated with HDCM or LDCM, as well as between parasites incubated with HDCM or UCM **(Table 1, Table S2).** Chromosomal mapping of all genes contained in the microarray indicated that transcriptional changes were broadly located throughout the genome (data not shown). Significant differential expression predominantly affected functional categories associated with transport, translation, protein binding and biosynthesis, antigenic variation, and mitochondrion/apicoplast (**Fig. 7A, Table S3, Table S4**). Real-time PCR analysis using primers specific for both asexual and sexual gene markers confirmed microarray findings for fifteen genes that were significantly up or downregulated (**Fig. 7B**).

Competitive gene set testing using correlation adjusted mean rank test (CAMERA) was performed to identify patterns of differential expression with respect to functional pathways and gene ontology classes [43]. Gene set testing for GO terms and metabolic pathways in HDCM-treated parasites revealed enrichment of gene sets associated with cytoskeletal rearrangements, antigenic variation, cytoadhesion, motor activity and ribosome biogenesis when compared to LDCM-treated parasites ($p < 0.01$, FDR < 0.05) **(Table 2, Table S5).** In contrast, HDCM induced downregulation of gene sets related to metabolic and cellular machinery, including apicoplast, endoplasmic reticulum, post-translational transport and export, and lipid metabolism ($p < 0.01$, FDR < 0.05)**.** Barcode plots of highly differentially expressed gene sets illustrate a strong pattern of enrichment and evident directionality (**Fig. 7C**).

Changes in specific gene sets related to cellular death mechanisms such as apoptosis, glycolysis, and autophagy were examined using rotation gene set testing for linear models (ROAST) (**Table 1, Table S6**) [44]. The apoptosis gene set exhibited significant changes in gene expression (n =

25, FDR = 1.35×10^{-6}), but this dysregulation was not found to be directional. Interestingly, the apoptosis-associated metacaspase gene *pfmc1* (PF3D7_1354800) was upregulated significantly at a low level (log2FC = 0.54, adj. p = 0.02), which was confirmed by RT-PCR analysis. Statistically significant, nondirectional dysregulation was also observed in genes encoding *Plasmodium* specific kinases (n = 130, FDR = 4.15×10^{-9})**.** In contrast, the glycolysis and autophagy gene sets were both significantly downregulated (n = 23, FDR = 1.19×10^{-3}; n = 6, FDR = 5.25×10^{-6}). Mitochondrial antioxidant and glutathione-associated gene sets were assessed to identify potential disruption of oxidative stress pathways. These exhibited significant downregulation (n = 10, FDR = 2.46×10^{-3}; n = 16, FDR = 8.24×10^{-4}).

Genes that are expressed in a clonally variant manner in *P. falciparum* include many that mediate the parasite's response to the host environment, *e.g.* invasion and sexual development [45]. Transcription of clonally variant genes would be expected to differ from the reference transcriptome, but not in a uniform direction. However, growth in HDCM induced significant upregulation (ROAST; FDR = 4.15×10^{-4}) of the variant expressed gene set from the 3D7 clone [46], suggesting that epigenetic mechanisms may have been affected (**Table 1**). These variant expressed genes are enriched with the heterochromatin marks H3K9me3 and *P. falciparum* heterochromatin protein 1 (PfHP1) [45,47,48]. High density CM induced significant upregulation of both sets of heterochromatin-marked genes (ROAST; H3K9me3: FDR = 1.52×10^{-3}; HP1: FDR = 2.11×10^{-3}), further suggesting that the HD environment alters gene regulatory chromatin structure.

To test the importance of glucose depletion in our transcriptome, we used CAMERA to assess whether genes associated with glucose deprivation are overrepresented in the high-density transcriptome. A panel of 184 *P. falciparum* genes was previously shown to be significantly dysregulated in an *in vitro* culture exposed to hypoglycemic conditions [22]. Competitive gene set testing for the high and low parasite density transcriptomes revealed no significant enrichment of the glucose deprivation gene set (p = 0.37, FDR = 0.37). Supplementation of LDCM with metabolic byproducts (LDCM+) and replenishment of HDCM with additional nutrients (HDCM+) revealed moderate effects on gene expression measured by RT-PCR when compared to microarray data for unsupplemented HDCM and LDCM. Differential expression in

a panel of 44 genes could not be entirely explained by starvation or waste accumulation, but rather a substantial proportion of gene responses behaved concordantly with microarray responses to high vs. low density (**Fig. 8, Table S7**). Genes associated with glucose deprivation were not significantly dysregulated under conditions of high density and high glucose.

Gametocyte signature

Analysis of a gene set exclusively comprised of gametocyte- or commitment-specific genes revealed an upregulation of sexual transcripts under HD conditions compared to LD conditions (ROAST; FDR = 4.92×10^{-2}) (**Fig. 9A, Table 1, Table S8, Table S9, Table S10**). Comparison of stage-specific gene expression obtained by cross-referencing the assembled gene panel with time course expression data from Young *et al.* revealed that early and middle stage gametocyte genes were predominantly affected **(Table 1)** [49]. A panel was assembled containing 36 genes that were either essential to gametocyte development, were known markers of gametocytogenesis, or had experimentally verified significance to gametocyte commitment or development. This panel was also upregulated under high-density conditions (ROAST; FDR = 3.11×10^{-3}) (**Fig. 9B, Table 1, Table S6**).

Transcriptional profiles from parasites exposed to HDCM, LDCM, and UCM were correlated to known transcriptional profiles corresponding to all intraerythrocytic stages of the parasite lifecycle. A published transcriptional time course encompassing the entire asexual and sexual blood-stage development of *P. falciparum* was used for the analysis [49]. Pearson correlations performed initially between biological replicates for high density, low density, and uninfected conditions revealed low biological variation ($r > 0.98$, $p < 0.0001$, $n = 3$). Subsequent Pearson correlation between experimental samples and the transcriptional time course revealed stronger correlation to late trophozoites rather than to committed or early gametocytes (LT; $0.74 < r < 0.77$ for all conditions, $p < 0.0001$) (**Fig. 9C**).

Discussion

High-density parasite cultures have a unique phenotypic signature

Data presented show that *P. falciparum* undergoes cell death in response to a high parasite density environment above $3x10^4$ parasites per microliter. Cell death can be initiated either in a high-density culture or during incubation in high-density conditioned medium but is never observed in a low parasite density environment. For this study, an *in vitro* culture system was adopted to isolate parasite behavior from host immune effects. Attempts to replicate *in vivo* conditions using normal human hematocrit at 40% proved unsustainable due to rapid consumption of glucose and production of lactic acid by uninfected red blood cells after 12 hours of incubation (**Fig. 5**). The death phenotype as defined above is different from the cell death modalities described in *P. falciparum* blood stages treated with antimalarial drugs [50–54], and is also morphologically distinct from autophagic-like cell death, crisis forms, and glucose-starved parasites, which rapidly shrink and die within the erythrocyte [22,37]. While aberrant parasites in high-density cultures shared similarities with apoptotic cells, they did not entirely conform to the conventional mammalian cell paradigm for programmed cell death or to other reports detailing programmed cell death in *Plasmodium* [55,56]. Interestingly, DNA fragmentation was never observed in the high-density parasites. A study by Engelbrecht *et al*. examining apoptosis-like regulated cell death in *P. falciparum* reported that parasites cultured at 3% parasitemia matured to late schizont stage but produced fewer merozoites, resulting in reduced replication rates. Furthermore, parasites underwent mitochondrial depolarization by 24hpi and DNA fragmentation by 48hpi [57]. In contrast, the parasite density of $3x10^4$ parasites per microliter used in our study is substantially higher than that used by Engelbrecht and colleagues, corresponding to 6% parasitemia. Dilution of HDCM to below 80% in complete culture media significantly diminished its killing activity, demonstrating that parasites cultured above or below a density of $2x10^4$ parasites per microliter exhibit differential behavior. Given the differences in methods for parasite culture, it is possible that exposure to varying conditions and density thresholds may induce distinctly different death phenotypes. Such observations have been made in *E. coli*, where the density-sensing factor EDF both mediates the MazEF death pathway and inhibits the apoptosis-like death (ALD) pathway [58]. In the case of *Plasmodium*, the manner in which parasites undergo cell death may not be singular or even linear in effect. There may be multiple unique markers for *Plasmodium* cell death, as is the case for other unicellular organisms [59].

High parasite density responses are independent of nutrient depletion and increased lactate

Neither the addition of excess glucose into the culture media nor a full replenishment of fresh culture media every 6 to 12 hours during incubation was sufficient to rescue high density cultures from growth inhibition and loss of viability in the following cycle, though glucose and media supplementation mitigated the loss of cell volume generally observed in high density cultures. Although frequent media changes could not restore viability in high-density cultures, late trophozoite stages but not schizonts could be rescued via dilution from high to low density, confirming that the observed cell death is indeed density-dependent as well as stage specific. The stage-specificity of killing activity by HDCM indicated that potential density sensing or signaling factors are likely to accumulate in the media during mature stage development. Whether these factors are byproducts of metabolic processes remains to be determined. Nutrient depletion was assessed by profiling of media components in HDCM, which revealed that essential amino acids and vitamins present in culture media were not significantly perturbed. Of all detectable components, only glucose was significantly depleted. Glucose and lactate were therefore selected for further analysis as the main signifiers of starvation and toxicity in high-density cultures.

Although glucose levels below the human hypoglycemic threshold were observed in HDCM and were independently shown to negatively affect parasite viability, gene set testing and validation by RT-PCR of nutrient-supplemented CM revealed that transcriptional responses to high density were not solely affected by dysregulation due to glucose starvation [22,43]. The continued consumption of glucose by high-density parasites even after cell death morphology had commenced may suggest that density-dependent death is a controlled process. Studies of apoptosis-like death by Ch'ng *et al* report that cellular death processes can continue for up to 10 hours after induction by chloroquine [60]. Linear modeling of glucose and HDCM titrations revealed different dynamic parasite responses with a threshold effect for HDCM induced death that was not observed for glucose depletion. We concluded that HDCM induced a more complex reaction than mere glucose starvation. The combined effect of glucose depletion and lactate supplementation on parasite cultures was not examined, as glucose depletion alone was already sufficient to cause a severe reduction in parasite growth and reinvasion whereas excess lactic acid had no effect.

The high density transcriptome is characterized by unusually broad effects and reveals stress but not sexual commitment

Exposure to high density induced a broad and unique transcriptional change overall, such that 16% of the genes present on the microarray were significantly differentially expressed. This percentage exceeds that of *C. albicans* (8.8%), *P. aeruginosa* (10%), and *E. coli* (6%) in response to environmental stressors, and is considerably higher than *P. falciparum* responses to antiparasitics such as chloroquine, antifolate, and choline analogs [5,24,50,52,61,62]. This unique high-density induced transcriptome contained elements of stress response, including upregulation of PfEMP1 genes and downregulation of translation and transport machinery [21–23]. Dysregulation of an essential kinase CRK1 (PF3D7_0417800) suggests major remodeling of downstream processes such as cell cycle control. Although the 2-hour incubation in HDCM promoted expression of sexual stage transcripts, this was insufficient to induce gametocytogenesis as determined by a 7-day culture. In fact, Pearson correlation coefficient analysis revealed that the expression pattern of parasites exposed to high-density environments correlated most highly with asexual trophozoites and not early gametocytes or committed mature stages, suggesting that the sexual development transcriptome undergoes a rapid dysregulation independent of sexual commitment under high-density conditions. Additionally, RT-PCR analysis of transcripts after supplementation of CM with nutrients and metabolic byproducts suggests that nutrient availability may have a strong impact on the expression of stage-specific transcripts. All together, these results highlight a novel transcriptional profile characteristic of density-dependent cell death, which is distinct from that of a sexually committed parasite.

Transcriptional responses to high density are associated with mechanisms of epigenetic control

The impetus for developmental decision-making, as in density sensing systems in unicellular populations, likely relies on communication between individuals through the release of signaling molecules that trigger coordinated responses. Our filtration assays precluded the possibility that the density-dependent death phenotype was the result of signaling via large secretory vesicles and suggested the presence of a small molecule in the culture medium at concentrations proportional to parasite density. As with density sensing molecules farnesol in yeast and SIF in

trypanosomes, soluble factors can indirectly lead to changes in parasite gene expression. In *P. falciparum*, induction of gametocytogenesis requires remodeling of the heterochromatic locus encoding the transcription factor ApiAP2G. Metabolic changes might affect the NADPH-dependent Sir2 histone deacetylases leading to chromatin remodeling and ApiAP2G activation. Interestingly, we have shown that variant expressed genes subject to epigenetic control were dysregulated in the high-density transcriptome. Epigenetic modifications have been shown to play a role in the activation of pathogenic processes such as invasion and cytoadherence, and have been proposed as a potential regulator of lifecycle transitions in *T. gondii* and *P. falciparum* [63–66].

Dysregulated metacaspase in high-density culture is linked to apoptotic-like mechanisms

P. falciparum exposed to high-density conditions exhibited hallmarks of oxidative stress and transcription of cell death pathways. These included mitochondrial injury, as evidenced by loss of membrane potential and downregulation of mitochondrial transcripts; shutdown of glutathione redox system and copper transporter transcripts; and downregulation of protein translation pathways. RT-PCR analysis confirmed the downregulation of an ubiquitin-activating enzyme (UBA1) (PF3D7_1333200) and a copper transporter-encoding gene CTR2 (PF3D7_1421900), as well as the upregulation of cytochrome c heme lyase (CCHL) (PF3D7_1224600). CCHL catalyzes the production of heme and cytochrome c, which are involved in oxidative stress and regulation of apoptosis, respectively [67]. Whereas *Plasmodium* sexual commitment has been widely studied, our results only begin to shed light on the density sensing pathways mediating cell death responses triggered by high-density parasite environments. *Plasmodium* cultured with drugs or at high densities have been shown to upregulate genes encoding cysteine proteases and metacaspases, respectively [55,60]. The yeast metacaspase YCA1 plays a pivotal role in activating apoptosis and its *Plasmodium* ortholog is a putative metacaspase with conserved caspase activity domains [68–70]. Accordingly, the *P. falciparum* metacaspase 1 gene MCA1 (PF3D7_1354800) was upregulated in parasites incubated in HDCM, suggesting that the response to high-density environments may involve a caspase-dependent cell death mechanism. Additionally, the phylogenetically conserved caspase and metacaspase substrate tudor staphylococcal nuclease (TSN) has been implicated in the caspase-mediated cell suicide pathway

in yeast and *Plasmodium* [71]. Further functional and metabolic studies are required to confirm these putative mechanisms underlying density-dependent cell death in *P. falciparum*.

A model for developmental decision-making: growth, sex or death?

We propose that high-density environments induce a unique death phenotype in *P. falciparum*, which has apoptotic-like features. This is consistent with other studies describing *Plasmodium* sexual commitment and density-dependent death in various microorganisms, where both sexual commitment and cell death are distinct developmental decisions undertaken as a response to varying external conditions [17,72–74]. In particular, the global transcriptional changes observed meet one of the criteria for a density-sensing system like quorum sensing in yeast. A model for *Plasmodium* decision-making would define the circumstances in which mature blood stages in a parasite population could progress through asexual development, convert to sexual development, or commit to death depending on the presence, absence or concentration of triggering signals in the surrounding environment. These signals may act synergistically with nutrient availability.

Identifying a mechanism for density-dependent cell death has the potential to unlock an entirely new area of research and provide a myriad of avenues for future investigation into a unique, alternative lifecycle decision in asexual *Plasmodium* parasites. Characterization of a signaling molecule and its relationship, if any, to caspase-dependent cell death pathways may lead to insights into parasite-mediated environmental sensing and variant-independent mechanisms of population regulation. These discoveries may consequently lead to greater understanding and control over parasite viability and infectivity while providing parasite-specific targets for intervention.

Materials and methods

Parasites and reagents

A cloned line of 3D7 was obtained from a gametocyte producing stabilate used for a genetic cross (D. Walliker). Chemical reagents were obtained from Sigma-Aldrich (St. Louis, MO USA) unless otherwise specified.

Parasite culture

P. falciparum asexual parasites were maintained *in vitro* as described with modification [29,75]. Cultures were maintained in type O+ sickle cell negative human erythrocytes suspended in 5% hematocrit in complete medium (RPMI 1640, pH 6.75 (Life Technologies, Grand Island, NY, USA), 25mM HEPES, 10 µg/ml gentamicin, 0.5mM hypoxanthine, 10% heat inactivated human serum and 25mM sodium bicarbonate). Cultures were incubated in a chamber with a gas environment of 5% CO_2, 1% O_2 and 94% N_2 at 37°C. Medium was replenished daily or as indicated and cultures were split frequently to maintain parasite density below $2x10^4$ parasites/µl or 4% parasitemia, until needed for assays. For experimental setups, late stage trophozoites and schizonts were isolated using gelatin flotation, Percoll enrichment, or heparin treatment as indicated for each assay (GE Life Sciences, Pittsburgh, PA USA; Sigma-Aldrich), followed by sorbitol synchronization of ring stages to within a 4-hour window.

High-density culture assays

For the 2-day high-density culture assay, synchronized starting cultures were obtained by harvesting late trophozoites and schizonts by centrifugation on a 40%/70% Percoll gradient, followed by sorbitol synchronization of ring stages no more than 4 hours after reinvasion. Starting cultures were diluted to $6x10^3$ parasites/µl for high density and $1x10^3$ parasites/µl for low density (1-1.5% and 0.2% parasitemia in 5% hematocrit), yielding ring stage parasites at $3x10^4$ and $5x10^3$ parasites/µl (6% and 1% parasitemia), respectively, in the following cycle. Parasite cultures at $3x10^4$ parasites/µl and $5x10^3$ parasites/µl were designated high density (HD) and low density (LD), respectively. HD and LD cultures were fed complete culture media during the late ring stage (~18hpi) and examined after 24 hours for morphological effects and after one full cycle for changes in viability. High-density culture assays were prepared in triplicate unless otherwise stated. For the 6-day growth assay, parasites were synchronized as described above. Ring stage parasites were seeded in duplicate at $5x10^3$ parasites/µl and maintained for 6 days with daily medium changes without subculturing.

Brightfield microscopy

Brightfield microscopy and image acquisition was performed on Giemsa-stained thin smears using a Nikon Labophot microscope (Nikon, Melville, NY USA). For parasitemia and differential stage counts, an Olympus BX41 microscope (Olympus, Center Valley, PA USA) was used. At least 1000 erythrocytes were counted to determine parasitemia. The proportions of different morphological stages were determined by counting 100 parasites. Freeman classification was used for parasite staging. "Aberrant parasites" are defined as shrunken, irregularly shaped, and highly dense in staining with compacted pigment at 40hpi, with or without release from the erythrocyte.

Volumetric analysis

Parasites were live-stained using BODIPY-ceramide TR (Sigma-Aldrich) and Hoechst 33342 (Thermo Fisher Scientific, Waltham, MA USA) for 2 hours prior to fixation and imaged on a DeltaVision Elite deconvolution microscope using the POL, TRITC and DAPI channels. Images were analyzed for spot detection and volumetric analysis using Volocity (Perkin Elmer, Waltham, MA USA). For high-density time points, n = 100+ parasites were imaged for volumetric analysis. For low-density time points 30-45hpi, n = 40+ parasites were imaged for volumetric analysis. At 50hpi, only 20 parasites in the low-density culture were imaged due to a substantial proportion of parasites having undergone merogony and reinvasion. Significant size differences between high and low density parasites were determined by one-way analysis of variance (ANOVA) and post-hoc analysis was performed using Tukey's honest significant difference test.

Mitochondria membrane potential (MMP) (Ψ_m) assay

The loss of MMP (Ψ_m) was assessed with JC-1 stain (Life Technologies, Grand Island, NY USA). For MMP staining, 6.5µg/ml (1 µM) JC-1 in modified complete medium (RPMI, 10% human serum) was added to cells at $5x10^5$ cells/µl one hour prior to each time point in 100µl volumes. Aliquots of 2-day cultures were pelleted, incubated with JC-1 stain preparation and washed. JC-1 positivity was calculated as the ratio of parasite population with JC-1 red-aggregate signal in polarized mitochondria (PE) to parasites with JC-1 green-accumulation signal (FITC) as determined by flow cytometry. A background level of JC-1 negativity less than 5% was observed in all samples. Significance between time points was determined by ANOVA and

Tukey's post-hoc test. Flow cytometry was performed on an Accuri C6 Flow Cytometer (BD Biosciences, Franklin Lakes, NJ USA) and analyzed with FlowJo v. 7.6.5 (Tree star, Ashland, OR USA). 10^5 total singlet cells were collected per sample. Side scatter was used to gate the singlet cell population used for all fluorescence analyses.

C32 binding assay

Parasite binding on C32 melanoma cells was carried out as described with changes [76,77]. Parasites were selected for adhesion to a C32 melanoma cell line (ATCC CRL 1585 C32r) as described. C32 cells were seeded onto coverslips at $5x10^4$ cells/ml 24 h prior to parasitized erythrocyte seeding and grown overnight. HD and LD cultures were prepared as described above, and binding assays were performed using late stage parasites collected 24 hours after the initial media change, following the appearance of aberrant morphology but prior to parasite release from the erythrocyte in HD cultures. Late stage parasites from both cultures were normalized to $6x10^3$ parasites/µl in 2% hematocrit, and 300µl of infected erythrocytes were added to C32 cells on coverslips and incubated at 37˚C for 90 min in standard gas environment. Coverslips were washed and fixed in 2% glutaraldehyde overnight at 4˚C. The number of parasites bound to 100 melanoma cells was determined using Giemsa stained smears.

In vitro parasite density threshold assay

Conditioned medium (CM) was harvested from trophozoites with densities in the range described in semi-immune children [25] and tested on low-density late trophozoites. For the harvest of CM, 27hpi trophozoite pellets were enriched using gelatin flotation and resuspended in complete medium. At 30hpi, trophozoites were seeded at the following parasite densities per 96 well: 10^4, 10^5, 10^6, 10^7 parasites/100 µl and incubated for 12 hours. CM was collected from each well and stored separately until use. 75µl of each CM was added undiluted to late trophozoites at $5x10^3$-$1x10^4$ parasites/µl and smears were taken after 12 hours of incubation for microscopy analysis. Control samples were treated with either complete culture medium or with UCM harvested after a 12-hour incubation on uninfected erythrocytes.

Harvest of parasite culture conditioned media

669 Parasites were prepared as for high and low-density culture assays and fed complete culture
670 medium at late ring stage. Cultures were incubated as described for 18-24 hours unless
671 otherwise indicated. CM was harvested by pelleting cultures at 1700rpm for 5 minutes and
672 collecting the supernatant. CM was then centrifuged at 4500rpm for 10 minutes to remove cell
673 and parasite debris and stored at 4°C for up to one week until use. Control UCM was harvested
674 after incubation for 18-24 hours with uninfected erythrocytes.
675
676 Conditioned medium assays
677 CM harvested as described above was added to late trophozoites (30hpi) at low density ($5x10^3$
678 parasites/µl). Cultures were assayed for morphological effects after 12 hours in CM (at schizont
679 stage) or after 24 hours to assess ring stage density and replication rate. Complete culture
680 medium or UCM harvested from uninfected erythrocytes were used as controls. Parasitemia and
681 differential counts were determined as described above. For stage-specific CM assays, CM
682 fractions were harvested from incubations spanning schizogony to 8hpi, 8-16hpi, 18-30hpi and
683 18-36hpi parasites in HD cultures in 150mm polystyrene petri dishes. Parasite cultures were
684 given fresh medium changes at 0hpi (schizogony/bursting), 8hpi, and 18hpi, respectively, and
685 collected as described at the end of each incubation period. Harvested CM was added to
686 synchronized low-density rings and incubated for 24 hours. Control samples were fed with
687 complete culture medium. For titration assay, CMs from high, low and uninfected erythrocyte
688 cultures were diluted in complete culture medium to 0, 20, 40, 60, 70, 80, 90, and 100% of
689 original CM concentrations. Titrations were added to low density, late trophozoites and
690 examined for aberrant morphology after 12 hours; n = 6. For the intra-isolate assay, test cultures
691 were synchronized as described above using *P. falciparum* isolates 3D7, Dd2, D6, HB3, and
692 1776. CM from 3D7 parasite cultures was added to low density test cultures for each of the
693 above isolates at late trophozoite stage. Ring parasitemia was measured after 24 hours. Control
694 samples were fed with complete culture medium. For all CM assays, Giemsa-stained thin blood
695 smears were examined by brightfield microscopy for parasitemia counts and changes in cell
696 morphology.
697
698 Mass spectrometry

Glucose and lactate analysis was performed at the Metabolomics Core Facility at Bio21 Institute. HD and LD cultures were prepared as described and fed fresh medium at 18hpi for subsequent incubation. Uninfected erythrocyte cultures were prepared at 5% hematocrit and 40% hematocrit. CM from all cultures was harvested at 6-hour time points over a 30-hour incubation and diluted 1:50 for analysis. Samples were added 1:1 with equal volumes of scyllo-inositol as a normalizing factor. Methoxyamine was added for ring expansion and samples were then derivatized using BSTFA-TCMS for gas chromatography mass spectrometry (GC-MS) analysis. Standard curves for lactic acid and glucose, respectively, were prepared in complete media.

To assess nutrient depletion in the HD and LD cultures, samples for liquid chromatography-mass spectrometry (LC-MS) analysis were prepared by adding 10µl of conditioned media into 390µl 80% acetonitrile/water to extract metabolites. Samples were incubated at 4 °C for 1 h on a vortex shaker. Samples were centrifuged 10' at 4000rpm to obtain a particle-free extract and stored at -80°C until analysis.

A Dionex RSLC U3000 LC system (Thermo) coupled with a high-resolution, Q-Exactive MS (Thermo) was used for analysis of medium components, as described elsewhere [78]. Briefly, 10µL sample was separated on a ZIC-pHILIC column (5µm, 4.6 by 150mm; Merck) over a 32 min gradient using 20mM ammonium carbonate (A) and acetonitrile (B) as mobile phases. The Q-Exactive MS was fitted with a heated electrospray source that switched between positive and negative modes. The mass resolution was 35,000 from *m/z* 85 to 1,050. A pooled quality control sample was analyzed periodically throughout the run to assess instrument drift. Analyte abundance was measured by LCMS peak height and identification of analytes was performed by matching accurate mass and retention time to authentic standards using the IDEOM software [79].

Nutrient replenishment and rescue assays

For glucose and lactate supplementation assays, HDCM and LDCM were supplemented with 0, 10, and 20mM glucose or 0, 20, and 40mM lactate. Supplemented CM was added to low-density late stage trophozoites and assessed for the density dependent death phenotype after 12 hours of incubation or for ring-stage reinvasion after 24 hours of incubation. For the glucose titration assay, a 1M stock solution of glucose was added to glucose-free RPMI to final concentrations of 0, 1, 2, 4, 6, 8, 10, and 11mM prior to preparation of culture media. Control treatments included

fresh complete medium or HDCM with and without 10mM additional glucose. Glucose titrations were added to low-density late trophozoites and assessed as for supplemented CM assays.

For medium replenishment assays, high and low density parasite cultures were prepared at late ring stage and measured for onset of the density-dependent death phenotype or loss of viability after 1 or 2 medium changes (18/30hpi, 18/24/26hpi, 18/30/36hpi, and 18/36/42hpi) or no medium change (control). At each time point, parasite cultures were spun at 300xg for 5 minutes, washed three times with complete medium and resuspended in fresh complete medium. Control cultures were pelleted and resuspended in original supernatant.

For subculture dilution assay, high-density parasite cultures were fed with fresh complete medium at late ring stage. At 30 and 42hpi, small volumes of each replicate were removed and washed twice in complete medium. Cell pellets were resuspended in fresh complete medium and uninfected erythrocytes to reduce the parasite density from $3x10^4$ parasites/µl to $5x10^3$ parasites/µl, or 1 in 6, keeping hematocrit constant. Control parasites were cultured at low density ($5x10^3$ parasites/µl) without dilution.

Glucose supplementation assay and flow cytometry

High and low density parasite cultures were prepared as described above (under High Density Culture Assays). At late ring stage (~18hpi), parasite cultures were fed with complete culture medium and supplemented with additional 20mM glucose for a final concentration of 30mM, or 3x normal concentration. Control cultures were not supplemented. Parasites were washed 3x after 24 hours of incubation at the nominal late schizont stage and nuclear content stained with 1uM SYTO 61 (Invitrogen, Carlsbad, CA USA) for 45 minutes at room temperature. Stained cells were washed an additional 3x and analyzed immediately on a BD FACSCanto (BD Biosciences, Franklin Lakes, NJ USA) using a far-red laser (excitation max 628 nm, emission max 645 nm). Mean fluorescent intensity was determined using FlowJo software (FlowJo LLC, Ashland OR USA). Significance was determined using Student's t-test.

Vesicle depletion

Filtration assays for vesicle depletion were performed using a Nalgene 100nm pore size PES filter filtration unit. Filtered and unfiltered CM was incubated on low-density late trophozoites. For all assays, parasites were assessed at schizont stage to quantify aberrant morphology and

induction of the density-dependent death phenotype. Ring stage density and replication rate was measured after 24 hours of incubation or following reinvasion.

Parasite culture for gene expression profiling

Low-density late stage trophozoites in two 150mm polystyrene plates (per replicate per condition) were treated with HDCM, LDCM or UCM for 2 hours prior to RNA harvest. This scale guaranteed adequate RNA yield for gene expression profiling as well as enabled high synchronicity of parasite cultures. A 2-hour treatment was selected to capture early transcriptional events associated with the phenotype.

RNA harvest and gene expression detection

Total RNA was harvested from the packed blood of *P. falciparum* 3D7 samples using TRIzol Reagent (Gibco, Gaithersburg, MD USA) as per manufacturer's instructions. RNA integrity was measured using an Agilent 2100 Bioanalyzer (Agilent, Santa Clara, CA USA) and samples with an RNA integrity number (RIN) of 6 and greater were hybridized to GeneChip® *Plasmodium/Anopheles* genome arrays (Affymetrix, Santa Clara, CA USA) in accordance to manufacturer's instructions.

Real-time RT-PCR

Sample RNA harvested from *P. falciparum* cultures was purified via the TRIzol method and used to synthesize 50ng/µl cDNA with the iScript cDNA Synthesis kit (Bio-Rad, Hercules, CA USA). Real-time PCR was prepared using approximately 100ng cDNA per sample with 2x Quantitect SYBR Green PCR Master Mix (Qiagen, Hilden, Germany) and 3 biological replicates were analyzed in triplicate on a Corbett Research Rotogene 3000 (Qiagen) (n = 9). Control samples containing no reverse transcriptase or no template DNA confirmed sample purity. Primers were designed using IDT PrimerQuest and run separately with optimized annealing temperatures. For CM supplementation, glucose and human serum were added to HDCM to 10mM and 5%, respectively (HDCM+). LDCM was supplemented with lactate and HDCM to 20mM and 1%, respectively (LDCM+). Cell cultures were incubated as described and 3 biological replicates of RNA were harvested per condition. Data was normalized against

housekeeping genes PF3D7_0307100 and PF3D7_1444800. Primer sequences used are included in the Supplemental material.

Microarray data analysis

Non-*Anopheles* probe-sets were pre-processed and expression measures were calculated using the GeneChip multi-array average (GCRMA) method [80]. The analysis was performed using R (version 2.15.0) [81] with the affy (version 1.34.0) and gcrma (version 2.28.0) packages that are part of the Bioconductor project [82]. The R package limma (version 3.12.0) [83] was used for calculation of differential expression by linear modeling and empirical Bayes statistics.

Gene set enrichment analysis was performed in R (version 2.15.0) using correlation adjusted mean rank gene set test (CAMERA). CAMERA is a competitive gene set test that compares members of a gene set to all members of the dataset, to determine whether transcripts differentially expressed under conditions of interest are overrepresented in the gene set, taking inter-gene associations into account [43]. GO-terms and gene descriptions were obtained from PlasmoDB (version 8.2) [84,85]. Additional gene sets (named PdBMET) were obtained from the website "Malaria parasite metabolic pathways" by Hagai Ginsburg (http://priweb.cc.huji.ac.il/malaria/). The autophagy, apoptosis, glycolysis and kinase gene sets were compiled from the Ginsburg website and recent literature [70,86–89]. Gametocyte specific genes were compiled from literature. Gene sets with nominal p-values less than 0.01 and false discovery rate (FDR) less than 0.05 were regarded as significant. Differential expression was determined by changes in transcript levels of 1.5-fold or greater when comparing between density samples. For assessing dysregulation of specific gene sets, significance and directionality of dysregulation were calculated using rotation gene set testing for linear models (ROAST) [44]. This method is a self contained gene set test that measures changes within an individual gene set as a whole by comparing the effect of different density conditions only on the genes within each set. For all comparisons, duplicates were removed and genes not available on the Affymetrix array were excluded from the analysis.

Statistical analysis

Statistical tests were applied as indicated. Significance between multiple populations was determined by one- or two-way ANOVA for one or two factors, respectively (Matlab:

822 Mathworks, MA USA), followed by Tukey's honest significant difference test for post-hoc
823 testing. Significance between two populations was determined by a two-tailed Student's t-test or
824 Welch's t-test and p-values were adjusted for multiple comparisons. Parasite responses to
825 HDCM versus glucose depletion were compared using linear regression modeling of cell death
826 as a function of media titration. HDCM and glucose-free culture medium were titrated via
827 dilution in complete culture medium from 100% to 0% and 11mM to 0mM, respectively.
828 Parasite death for both conditions was calculated as percent loss of growth compared to
829 uninhibited growth in control samples and log transformed for linear regression. For comparison
830 of parasite responses to both treatments, we performed a global fit for the combined data
831 resulting from both treatments and used ANOVA to calculate the probability of the variance
832 arising from the global fit. The significance test resulting in p-value < 0.05 favored a more
833 complex model with two linear regression models fitted to each data set over the null hypothesis
834 with a single linear regression model [90]. For all comparisons, adjusted p-values of less than
835 0.05 were considered statistically significant. For gene set analysis (CAMERA, ROAST), FDR
836 values of less than 0.05 were considered statistically significant. Error bars indicate standard
837 error for differences between two populations.
838
839 Gametocyte transcript analysis
840 A panel of 711 genes was assembled from the literature. The resulting panel included genes
841 associated with gametocytogenesis by correlation, expression profiling, or functional analysis.
842 532 of these 711 genes were present on the Affymetrix microarray. Upregulated and
843 downregulated genes were classified with ontology annotations gathered from the PlasmoDB
844 website. An additional panel of 36 gametocyte "marker" genes was assembled from published
845 literature, including known signifiers of specific sexual stages (*i.e. pfs16, pfg377*) as well as
846 putative inducers of gametocytogenesis (*i.e. pfgig, pfgdv1*) that have been confirmed and
847 validated using *in vivo* experimentation, such as gene knockdown and other molecular and
848 cellular assays. Heat maps were generated with Broad Institute software using ranked
849 gametocyte gene expression values from microarray analysis [91]. Transcriptional signatures
850 from each experimental condition were compared with those of various stages in asexual and
851 gametocyte development as in Young *et al* [49]. Pearson correlation coefficients were calculated
852 for the transcriptional profiles for all experimental conditions using R (version 2.15.0).

Gametocyte culture assay

HDCM, LDCM, and UCM were harvested as described previously. Low-density trophozoites were synchronized as for gene profiling assay. At 33hpi on Day 0, cultures were washed twice in RPMI and replated in HDCM, LDCM, UCM or complete culture media, in triplicate for each condition. Samples were incubated for 2h at 37C, washed 3x in RPMI, and then replated in complete culture media for gametocyte culture. CM-treated cultures were fed daily with standard culture media and sorbitol synchronized on Days 1, 2 and 3 to remove asexual stages from culture. On Day 7, samples were stained with thiazole orange (Sigma, 1:10,000) and measured for gametocytemia by flow cytometry. Data was analyzed using FlowJo software. For each condition, mean and standard error was computed. The difference between means was calculated using one-way ANOVA with Tukey's post-hoc test.

Acknowledgements

We thank Mr. Michael Cammer for his image processing expertise, Dr. Ute Frevert for microscope use, Ms. Maria Carolina Bermudez for help in parasite culture, Dr. Leann Tilley for use of culture, imaging and cytometry equipment and Drs. Manuel Llinas, Ian Hastings, Bjorn Kafsack, and Matt Dixon for insightful experimental advice.

We thank Wellcome Trust Programme Grant No.041354, Ellison Foundation, CV Starr Foundation and Burroughs Wellcome Fund, and National Institutes of Health grant AI084156 funding awarded to K.P.D. for salary support for K.P.D., A.L.S., T.R., and S.A.

With thanks to the Biological Optical Microscopy Platform at the University of Melbourne for access to microscopy equipment and software licensing.

The authors acknowledge the facilities and the scientific and technical assistance of the Metabolomics Australia Facility at Bio21 Institute, the University of Melbourne.

Author contributions

K.P.D. conceived the study. All co-authors contributed to aspects of experimental design and data analysis. E.S.C., S.Z.A, M.T. and K.P.D. planned experiments. E.S.C, S.Z.A., M.T., A.L.S., S.A.C., K.S.S., and A.E.S. performed experiments. K.S.S., D.J.C., J.P.D., M.F.D., and K.P.D. contributed reagents and other essential material. E.S.C., S.Z.A., T.S.R., G.Q.T., A.E.S., and D.J.C. analyzed data. All co-authors contributed to writing the paper. E.S.C., M.F.D., and K.P.D. prepared the manuscript. K.P.D., M.F.D., and J.P.D. gave final approval for publication.

References

1. Bruce MC & Day KP (2002) Cross-species regulation of malaria parasitaemia in the human host. *Curr. Opin. Microbiol.* **5**, 431–437.

2. Imrie H, Fowkes FJI, Michon P, Tavul L, Reeder JC & Day KP (2007) Low prevalence of an acute phase response in asymptomatic children from a malaria-endemic area of Papua New Guinea. *Am. J. Trop. Med. Hyg.* **76**, 280–4.

3. Brown KN (1990) The parasitology of malaria and the study of protective immunity. *Immunol. Lett.* **25**, 97–9.

4. Miller MB & Bassler BL (2001) Quorum sensing in bacteria. *Annu. Rev. Microbiol.* **55**, 165–99.

5. Wagner VE, Bushnell D, Passador L, Brooks AI & Iglewski BH (2003) Microarray analysis of Pseudomonas aeruginosa quorum-sensing regulons: effects of growth phase and environment. *J. Bacteriol.* **185**, 2080–95.

6. Schmitt MJ & Breinig F (2006) Yeast viral killer toxins: lethality and self-protection. *Nat. Rev. Microbiol.* **4**, 212–21.

7. Severin FF & Hyman AA (2002) Pheromone Induces Programmed Cell Death in S . cerevisiae. *Curr. Biol.* **12**, 233–235.

8. Chen H, Fujita M, Feng Q, Clardy J & Fink GR (2004) Tyrosol is a quorum-sensing molecule in Candida albicans. *Proc. Natl. Acad. Sci. U. S. A.* **101**, 5048–52.

9. Deveau A, Piispanen AE, Jackson AA & Hogan DA (2010) Farnesol induces hydrogen peroxide resistance in Candida albicans yeast by inhibiting the Ras-cyclic AMP signaling pathway. *Eukaryot. Cell* **9**, 569–77.

10. Hornby JM, Jensen EC, Lisec AD, Tasto JJ, Jahnke B, Shoemaker R, Dussault P & Nickerson KW (2001) Quorum sensing in the dimorphic fungus Candida albicans is mediated by farnesol. *Appl. Environ. Microbiol.* **67**, 2982–92.

11. Zhu J, Krom BP, Sanglard D, Intapa C, Dawson CC, Peters BM, Shirtliff ME & Jabra-Rizk MA (2011) Farnesol-induced apoptosis in Candida albicans is mediated by Cdr1-p extrusion and depletion of intracellular glutathione. *PLoS One* **6**, e28830.

12. Reuner B, Vassella E, Yutzy B & Boshart M (1997) Cell density triggers slender to stumpy differentiation of Trypanosoma brucei bloodstream forms in culture. *Mol. Biochem. Parasitol.* **90**, 269–80.

13. Tagoe DNA, Kalejaiye TD & de Koning HP (2015) The ever unfolding story of cAMP signaling in trypanosomatids: Vive la difference! *Front. Pharmacol.* **6**, 1–13.

14. Mony BM, MacGregor P, Ivens A, Rojas F, Cowton A, Young J, Horn D & Matthews K (2013) Genome-wide dissection of the quorum sensing signalling pathway in Trypanosoma brucei . *Nature* **505**, 1–17.

15. Carter R & Miller LH (1979) Evidence for environmental modulation of gametocytogenesis in Plasmodium falciparum in continuous culture. *Bull. World Health Organ.* **57 Suppl 1**, 37–52.

16. Williams J (1999) Stimulation of Plasmodium falciparum gametocytogenesis by conditioned medium from parasite cultures. *Am. J. Trop. Med. Hyg.* **60**, 7–13.

17. Dyer M & Day KP (2003) Regulation of the rate of asexual growth and commitment to sexual development by diffusible factors from in vitro cultures of Plasmodium falciparum. *Am. J. Trop. Med. Hyg.* **68**, 403–409.

18. Fivelman QL, McRobert L, Sharp S, Taylor CJ, Saeed M, Swales CA, Sutherland CJ &

934 Baker DA (2007) Improved synchronous production of Plasmodium falciparum
935 gametocytes in vitro. *Mol. Biochem. Parasitol.* **154**, 119–123.

936 19. Carter LM, Kafsack BFC, Llinás M, Mideo N, Pollitt LC & Reece SE (2013) Stress and sex
937 in malaria parasites: Why does commitment vary? *Evol. Med. public Heal.* **2013**, 135–47.

938 20. Mantel PY, Hoang AN, Goldowitz I, Potashnikova D, Hamza B, Vorobjev I, Ghiran I, Toner
939 M, Irimia D, Ivanov AR, Barteneva N & Marti M (2013) Malaria-infected erythrocyte-
940 derived microvesicles mediate cellular communication within the parasite population and
941 with the host immune system. *Cell Host Microbe* **13**, 521–534.

942 21. Oakley MSM, Kumar S, Anantharaman V, Zheng H, Mahajan B, Haynes JD, Moch JK,
943 Fairhurst R, McCutchan TF & Aravind L (2007) Molecular factors and biochemical
944 pathways induced by febrile temperature in intraerythrocytic Plasmodium falciparum
945 parasites. *Infect. Immun.* **75**, 2012–2025.

946 22. Fang J, Zhou H, Rathore D, Sullivan M, Su X-Z & McCutchan TF (2004) Ambient glucose
947 concentration and gene expression in Plasmodium falciparum. *Mol. Biochem. Parasitol.*
948 **133**, 125–129.

949 23. Babbitt SE, Altenhofen L, Cobbold SA, Istvan ES, Fennell C, Doerig C, Llinas M &
950 Goldberg DE (2012) Plasmodium falciparum responds to amino acid starvation by entering
951 into a hibernatory state. *Proc. Natl. Acad. Sci.* **109**, E3278–87.

952 24. Gunasekera AM, Myrick A, Le Roch K, Winzeler E & Wirth DF (2007) Plasmodium
953 falciparum: genome wide perturbations in transcript profiles among mixed stage cultures
954 after chloroquine treatment. *Exp. Parasitol.* **117**, 87–92.

955 25. Bruce MC, Donnelly CA, Alpers MP, Galinski MR, Barnwell JW, Walliker D & Day KP
956 (2000) Cross-species interactions between malaria parasites in humans. *Science* **287**, 845–
957 848.

958 26. Albuquerque P, Nicola AM, Nieves E, Paes HC, Williamson PR, Silva-Pereira I &
959 Casadevall A (2014) Quorum sensing-mediated, cell density-dependent regulation of
960 growth and virulence in Cryptococcus neoformans. *MBio* **5**, e00986–13.

27. Bruce MC, Donnelly CA, Packer M, Lagog M, Gibson N, Narara A, Walliker D, Alpers MP & Day KP (2000) Age- and species-specific duration of infection in asymptomatic malaria infections in Papua New Guinea. *Parasitology* **121**, 247–256.

28. White NJ, Chapman D & Watt G (1992) The effects of multiplication and synchronicity on the vascular distribution of parasites in falciparum malaria. *Trans. R. Soc. Trop. Med. Hyg.* **86**, 590–7.

29. Trager W & Jensen JB (1976) Human malaria parasites in continuous culture. *Science (80-.).*, 673–675.

30. Kwiatkowski D (1989) Febrile temperatures can synchronize the growth of Plasmodium falciparum in vitro. *J. Exp. Med.* **169**, 357–61.

31. Färnert A (2008) Plasmodium falciparum population dynamics: only snapshots in time? *Trends Parasitol.* **24**, 340–344.

32. Koyama FC, Chakrabarti D & Garcia CRS (2009) Molecular machinery of signal transduction and cell cycle regulation in Plasmodium. *Mol. Biochem. Parasitol.* **165**, 1–7.

33. Francis SE, Sullivan DJJ & Glodberg DE (1997) Hemoglobin metabolism in the malaria parasite Plasmodium falciparum. *Annu. Rev. Microbiol.* **51**, 97–123.

34. Bozdech Z, Llinás M, Pulliam BL, Wong ED, Zhu J & DeRisi JL (2003) The transcriptome of the intraerythrocytic developmental cycle of Plasmodium falciparum. *PLoS Biol.* **1**, E5.

35. Schnitzer B, Sodeman T, Mead ML & Contacos PG (1972) Pitting function of the spleen in malaria: ultrastructural observations. *Science* **177**, 175–7.

36. Pereira C, Camougrand N, Manon S, Sousa MJ & Côrte-Real M (2007) ADP/ATP carrier is required for mitochondrial outer membrane permeabilization and cytochrome c release in yeast apoptosis. *Mol. Microbiol.* **66**, 571–582.

37. Jensen MD, Conley M & Helstowski LD (1983) Culture of Plasmodium falciparum: the role of pH, glucose, and lactate. *J. Parasitol.* **69**, 1060–1067.

38. Zolg J, Macleod A, Scaife J & Beaudoin R (1984) The accumulation of lactic acid and its influence on the growth ofPlasmodium falciparum in synchronized cultures. *In Vitro* **20**, 205–215.

39. Divo AA, Geary TG, Davis NL & Jensen JB (1985) Nutritional requirements of Plasmodium falciparum in culture. I. Exogenously supplied dialyzable components necessary for continuous growth. *J. Protozool.* **32**, 59–64.

40. Liu J, Istvan ES, Gluzman IY, Gross J & Goldberg DE (2006) Plasmodium falciparum ensures its amino acid supply with multiple acquisition pathways and redundant proteolytic enzyme systems. *Proc. Natl. Acad. Sci. U. S. A.* **103**, 8840–5.

41. Regev-Rudzki N, Wilson DW, Carvalho TG, Sisquella X, Coleman BM, Rug M, Bursac D, Angrisano F, Gee M, Hill AF, Baum J & Cowman AF (2013) Cell-cell communication between malaria-infected red blood cells via exosome-like vesicles. *Cell* **153**, 1120–1133.

42. Nogueira F, Diez A, Radfar A, Pérez-Benavente S, Rosario VE Do, Puyet A & Bautista JM (2010) Early transcriptional response to chloroquine of the Plasmodium falciparum antioxidant defence in sensitive and resistant clones. *Acta Trop.* **114**, 109–115.

43. Wu D & Smyth GK (2012) Camera: a competitive gene set test accounting for inter-gene correlation. *Nucleic Acids Res.* **40**, e133–e133.

44. Wu D, Lim E, Vaillant F, Asselin-Labat M-L, Visvader JE & Smyth GK (2010) ROAST: rotation gene set tests for complex microarray experiments. *Bioinformatics* **26**, 2176–82.

45. Flueck C, Bartfai R, Volz J, Niederwieser I, Salcedo-Amaya AM, Alako BTF, Ehlgen F, Ralph SA, Cowman AF, Bozdech Z, Stunnenberg HG & Voss TS (2009) Plasmodium falciparum heterochromatin protein 1 marks genomic loci linked to phenotypic variation of exported virulence factors. *PLoS Pathog.* **5**, e1000569.

46. Rovira-Graells N, Gupta AP, Planet E, Crowley VM, Mok S, Ribas de Pouplana L, Preiser PR, Bozdech Z & Cortés A (2012) Transcriptional variation in the malaria parasite Plasmodium falciparum. *Genome Res.* **22**, 925–38.

1012 47. Lopez-Rubio JJ, Mancio-Silva L & Scherf A (2009) Genome-wide analysis of
1013 heterochromatin associates clonally variant gene regulation with perinuclear repressive
1014 centers in malaria parasites. *Cell Host Microbe* **5**, 179–90.

1015 48. Salcedo-Amaya AM, van Driel MA, Alako BT, Trelle MB, van den Elzen AMG, Cohen AM,
1016 Janssen-Megens EM, van de Vegte-Bolmer M, Selzer RR, Iniguez AL, Green RD,
1017 Sauerwein RW, Jensen ON & Stunnenberg HG (2009) Dynamic histone H3 epigenome
1018 marking during the intraerythrocytic cycle of Plasmodium falciparum. *Proc. Natl. Acad.*
1019 *Sci. U. S. A.* **106**, 9655–60.

1020 49. Young JA, Fivelman QL, Blair PL, De La Vega P, Le Roch KG, Zhou Y, Carucci DJ, Baker
1021 DA & Winzeler EA (2005) The Plasmodium falciparum sexual development transcriptome:
1022 A microarray analysis using ontology-based pattern identification. *Mol. Biochem. Parasitol.*
1023 **143**, 67–79.

1024 50. Ganesan K, Ponmee N, Jiang L, Fowble JW, White J, Kamchonwongpaisan S, Yuthavong Y,
1025 Wilairat P & Rathod PK (2008) A genetically hard-wired metabolic transcriptome in
1026 Plasmodium falciparum fails to mount protective responses to lethal antifolates. *PLoS*
1027 *Pathog.* **4**, e1000214.

1028 51. Klonis N, Crespo-Ortiz MP, Bottova I, Abu-Bakar N, Kenny S, Rosenthal PJ & Tilley L
1029 (2011) Artemisinin activity against Plasmodium falciparum requires hemoglobin uptake and
1030 digestion. *Proc. Natl. Acad. Sci. U. S. A.* **108**, 11405–10.

1031 52. Le Roch KG, Johnson JR, Ahiboh H, Chung D-WD, Prudhomme J, Plouffe D, Henson K,
1032 Zhou Y, Witola W, Yates JR, Mamoun C Ben, Winzeler EA & Vial H (2008) A systematic
1033 approach to understand the mechanism of action of the bisthiazolium compound T4 on the
1034 human malaria parasite, Plasmodium falciparum. *BMC Genomics* **9**, 513.

1035 53. Totino PRR, Daniel-Ribeiro CT, Corte-Real S & Ferreira-da-Cruz M de F (2008)
1036 Plasmodium falciparum: Erythrocytic stages die by autophagic-like cell death under drug
1037 pressure. *Exp. Parasitol.* **118**, 478–486.

1038 54. Nyakeriga AM, Perlmann H, Hagstedt M, Berzins K, Troye-Blomberg M, Zhivotovsky B,

1039 Perlmann P & Grandien A (2006) Drug-induced death of the asexual blood stages of
1040 Plasmodium falciparum occurs without typical signs of apoptosis. *Microbes Infect.* **8**, 1560–
1041 1568.

1042 55. Mutai BK & Waitumbi JN (2010) Apoptosis stalks Plasmodium falciparum maintained in
1043 continuous culture condition. *Malar. J.* **9**, S6.

1044 56. Al-Olayan EM, Williams GT & Hurd H (2002) Apoptosis in the malaria protozoan,
1045 Plasmodium berghei: a possible mechanism for limiting intensity of infection in the
1046 mosquito. *Int. J. Parasitol.* **32**, 1133–43.

1047 57. Engelbrecht D & Coetzer TL (2016) Plasmodium falciparum exhibits markers of regulated
1048 cell death at high population density in vitro. *Parasitol. Int.* **65**, 715–727.

1049 58. Erental A, Sharon I, Engelberg-Kulka H, Sandler HA & Rosenberg SM (2012) Two
1050 Programmed Cell Death Systems in Escherichia coli: An Apoptotic-Like Death Is Inhibited
1051 by the mazEF-Mediated Death Pathway. *PLoS Biol.* **10**, e1001281.

1052 59. Carmona-Gutierrez D, Eisenberg T, Büttner S, Meisinger C, Kroemer G & Madeo F (2010)
1053 Apoptosis in yeast: triggers, pathways, subroutines. *Cell Death Differ.* **17**, 763–73.

1054 60. Ch'ng J-H, Kotturi SR, Chong AG-L, Lear MJ & Tan KS-W (2010) A programmed cell
1055 death pathway in the malaria parasite Plasmodium falciparum has general features of
1056 mammalian apoptosis but is mediated by clan CA cysteine proteases. *Cell Death Dis.* **1**,
1057 e26.

1058 61. Cao Y-Y, Cao Y-B, Xu Z, Ying K, Li Y, Xie Y, Zhu Z-Y, Chen W-S & Jiang Y-Y (2005)
1059 cDNA microarray analysis of differential gene expression in Candida albicans biofilm
1060 exposed to farnesol. *Antimicrob. Agents Chemother.* **49**, 584–9.

1061 62. DeLisa MP, Wu CF, Wang L, Valdes JJ & Bentley WE (2001) DNA microarray-based
1062 identification of genes controlled by autoinducer 2-stimulated quorum sensing in
1063 Escherichia coli. *J. Bacteriol.* **183**, 5239–47.

1064 63. Cortés A, Carret C, Kaneko O, Yim Lim BYS, Ivens A & Holder AA (2007) Epigenetic

1065 silencing of Plasmodium falciparum genes linked to erythrocyte invasion. *PLoS Pathog.* **3**,
1066 1023–1035.

1067 64. Saksouk N, Bhatti MM, Kieffer S, Aaron T, Musset K, Garin J, Jr WJS, Hakimi M & Smith
1068 AT (2005) Histone-Modifying Complexes Regulate Gene Expression Pertinent to the
1069 Differentiation of the Protozoan Parasite Toxoplasma gondii Histone-Modifying Complexes
1070 Regulate Gene Expression Pertinent to the Differentiation of the Protozoan Parasite
1071 Toxoplasma go. *Mol. Cell. Biol.* **25**, 10301–10314.

1072 65. Bougdour A, Maubon D, Baldacci P, Ortet P, Bastien O, Bouillon A, Barale J-C, Pelloux H,
1073 Ménard R & Hakimi M-A (2009) Drug inhibition of HDAC3 and epigenetic control of
1074 differentiation in Apicomplexa parasites. *J. Exp. Med.* **206**, 953–66.

1075 66. Sinha A, Hughes KR, Modrzynska KK, Otto TD, Pfander C, Dickens NJ, Religa AA,
1076 Bushell E, Graham AL, Cameron R, Kafsack BFC, Williams AE, Llinás M, Berriman M,
1077 Billker O & Waters AP (2014) A cascade of DNA-binding proteins for sexual commitment
1078 and development in Plasmodium. *Nature* **507**, 253–7.

1079 67. Percário S, Moreira DR, Gomes B a Q, Ferreira MES, Gonçalves ACM, Laurindo PSOC,
1080 Vilhena TC, Dolabela MF & Green MD (2012) Oxidative stress in malaria. *Int. J. Mol. Sci.*
1081 **13**, 16346–72.

1082 68. Mazzoni C & Falcone C (2008) Caspase-dependent apoptosis in yeast. *Biochim. Biophys.*
1083 *Acta* **1783**, 1320–7.

1084 69. Bettiga M, Calzari L, Orlandi I, Alberghina L & Vai M (2004) Involvement of the yeast
1085 metacaspase Yca1 in ubp10Delta-programmed cell death. *FEMS Yeast Res.* **5**, 141–7.

1086 70. Meslin B, Barnadas C, Boni V, Latour C, De Monbrison F, Kaiser K & Picot S (2007)
1087 Features of apoptosis in Plasmodium falciparum erythrocytic stage through a putative role
1088 of PfMCA1 metacaspase-like protein. *J. Infect. Dis.* **195**, 1852–1859.

1089 71. Sundström JF, Vaculova A, Smertenko AP, Savenkov EI, Golovko A, Minina E, Tiwari BS,
1090 Rodriguez-Nieto S, Zamyatnin AA, Välineva T, Saarikettu J, Frilander MJ, Suarez MF,
1091 Zavialov A, Ståhl U, Hussey PJ, Silvennoinen O, Sundberg E, Zhivotovsky B & Bozhkov P

V (2009) Tudor staphylococcal nuclease is an evolutionarily conserved component of the programmed cell death degradome. *Nat. Cell Biol.* **11**, 1347–54.

72. Reece SE, Pollitt LC, Colegrave N & Gardner A (2011) The meaning of death: Evolution and ecology of apoptosis in protozoan parasites. *PLoS Pathog.* **7**, 1–10.

73. Taylor-Brown E & Hurd H (2013) The first suicides: a legacy inherited by parasitic protozoans from prokaryote ancestors. *Parasit. Vectors* **6**, 108.

74. Ali M, Al-Olayan EM, Lewis S, Matthews H & Hurd H (2010) Naturally occurring triggers that induce apoptosis-like programmed cell death in Plasmodium berghei ookinetes. *PLoS One* **5**.

75. Day KP, Karamalis F, Thompson J, Barnes DA, Peterson C, Brown H, Brown G V & Kemp DJ (1993) Genes necessary for expression of a virulence determinant and for transmission of Plasmodium falciparum are located on a 0.3-megabase region of chromosome 9. *Proc. Natl. Acad. Sci. U. S. A.* **90**, 8292–6.

76. Biggs BA, Gooze L, Wycherley K, Wilkinson D, Boyd AW, Forsyth KP, Edelman L, Brown G V & Leech JH (1990) Knob-independent cytoadherence of Plasmodium falciparum to the leukocyte differentiation antigen CD36. *J. Exp. Med.* **171**, 1883–1892.

77. Piper K, Roberts D & Day K (1999) Plasmodium falciparum: Analysis of the Antibody Specificity to the Surface of the Trophozoite-Infected Erythrocyte. *Exp. Parasitol.* **91**, 161–169.

78. Creek DJ, Chua HH, Cobbold SA, Nijagal B, Macrae JI, Dickerman BK, Gilson PR, Ralph SA & McConville MJ (2016) Metabolomics-based screening of the Malaria Box reveals both novel and established mechanisms of action. *Antimicrob. Agents Chemother.*, AAC.01226–16.

79. Creek DJ, Jankevics A, Burgess KE V., Breitling R & Barrett MP (2012) IDEOM: an Excel interface for analysis of LC–MS-based metabolomics data. *Bioinformatics* **28**, 1048–1049.

80. Wu Z, Irizarry RA, Gentleman R, Martinez-Murillo F & Spencer F (2004) A Model-Based

Background Adjustment for Oligonucleotide Expression Arrays. *J. Am. Stat. Assoc.* **99**, 909–917.

81. R Core Team (2013). R: A language and environment for statistical computing. R Foundation for Statistical Computing, Vienna, Austria. URL http://www.R-project.org/.

82. Gentleman RC, Carey VJ, Bates DM, Bolstad B, Dettling M, Dudoit S, Ellis B, Gautier L, Ge Y, Gentry J, Hornik K, Hothorn T, Huber W, Iacus S, Irizarry R, Leisch F, Li C, Maechler M, Rossini AJ, Sawitzki G, Smith C, Smyth G, Tierney L, Yang JYH & Zhang J (2004) Bioconductor : open software development for computational biology and bioinformatics. *Genome Biol.* **5**.

83. Smyth GK (2004) Linear Models and Empirical Bayes Methods for Assessing Differential Expression in Microarray. *Stat. Appl. Genet. Mol. Biol.* **3**, 1–26.

84. Ashburner M, Ball CA, Blake JA, Botstein D, Butler H, Cherry JM, Davis AP, Dolinski K, Dwight SS, Eppig JT, Harris MA, Hill DP, Issel-Tarver L, Kasarskis A, Lewis S, Matese JC, Richardson JE, Ringwald M, Rubin GM & Sherlock G (2000) Gene Ontology: tool for the unification of biology. *Nat. Genet.* **25**, 25–29.

85. Aurrecoechea C, Brestelli J, Brunk BP, Dommer J, Fischer S, Gajria B, Gao X, Gingle A, Grant G, Harb OS, Heiges M, Innamorato F, Iodice J, Kissinger JC, Kraemer E, Li W, Miller JA, Nayak V, Pennington C, Pinney DF, Roos DS, Ross C, Stoeckert CJ, Treatman C & Wang H (2009) PlasmoDB: a functional genomic database for malaria parasites. *Nucleic Acids Res.* **37**, D539–D543.

86. Brennand A, Gualdrón-López M, Coppens I, Rigden DJ, Ginger ML & Michels PAM (2011) Autophagy in parasitic protists: unique features and drug targets. *Mol. Biochem. Parasitol.* **177**, 83–99.

87. Engelbrecht D, Durand PM & Coetzer TL (2012) On Programmed Cell Death in Plasmodium falciparum: Status Quo. *J. Trop. Med.* **2012**, 646534.

88. Guha M, Choubey V, Maity P, Kumar S, Shrivastava K, Puri SK & Bandyopadhyay U (2007) Overexpression, purification and localization of apoptosis related protein from

Plasmodium falciparum. *Protein Expr. Purif.* **52**, 363–372.

89. Ward P, Equinet L, Packer J & Doerig C (2004) Protein kinases of the human malaria parasite Plasmodium falciparum: the kinome of a divergent eukaryote. *BMC Genomics* **5**, 79.

90. Motulsky HJ & Christopoulos A (2003) Fitting models to biological data using linear and nonlinear regression: a practical guide to curve fitting. *GraphPad Softw. Inc., San Diego CA, www.graphpad.com.*

91. Kuehn H, Liberzon A, Reich M & Mesirov JP (2008) Using GenePattern for gene expression analysis. *Curr. Protoc. Bioinformatics* **Chapter 7**, Unit 7.12.

Supporting information:

Table S1. Comparison of essential media components in high vs. low density conditioned medium

Table S2: Summary of global changes in gene expression, high vs. low density; high density vs. uninfected

Table S3. Microarray expression values for top 50 genes with significant differential expression, high vs. low density

Table S4: Microarray expression values for all genes with significant differential expression, high vs. low density

Table S5. Gene set enrichment profiles, high vs. low density

Table S6. Microarray expression values for gene sets used in mROAST analysis, high vs. low density

Table S7. Validation of genes by RT-PCR with nutrient-supplemented HDCM+ and LDCM+

Table S8. List of gametocyte-associated genes and accompanying references, all compiled (711)

Table S9. Source literature for gametocyte stage-associated genes, all compiled (711)

Table S10. Microarray expression values for gametocyte-associated genes, full panel (532), high vs. low density

Table S11. RT-PCR Primer sequences

Figure Legends

Figure 1. *P. falciparum* growth is inhibited at high densities. (A) Parasite density and (B) differential count was measured over 6 days of growth with no subculturing. Counts were averaged over all replicates and presented as parasite density per microliter of culture. R: rings; T: trophozoites; S: schizonts. "Aberrant" indicates parasites that are shrunken, irregularly shaped, and highly dense in staining with compacted pigment. "Released" refers to parasites that are not contained within an erythrocyte and do not contribute to parasitemia. Mean ± SEM. n = 3.

Figure 2. High-density parasite cultures exhibit aberrant morphology. (A) Schematic of high-density culture set up. High and low-density parasites are fed at late ring stage and incubated for 18h until late trophozoite stage. Morphology is assessed throughout late trophozoite and schizont stage, or 18-30h after initial feeding. (B,C) Brightfield microscopy of low parasite density (LD) and high parasite density (HD) cultures illustrates a unique death phenotype. (B) LD parasites undergo normal development while HD parasites exhibit inhibition of schizont maturation and merogony, cell shrinking, blebbing and release of parasites from erythrocytes. Scale bar, 5μm. Differential counts (C) are shown as proportions out of 100 infected erythrocytes (iRBC) and averaged over replicates (n = 3). R: rings; T: trophozoites; S: schizonts. "Aberrant" indicates parasites that are shrunken, irregularly shaped, and highly dense in staining with compacted pigment. (D) Volumetric analysis of HD and LD parasites shows inhibited late stage development in HD parasites. For HD parasites, n >= 100 for all time points; for LD parasites, n >= 40 at 30-45hpi and n = 20 at 50hpi. (E) Loss of mitochondrial membrane potential in high-density parasites is shown as the percentage of parasites with JC-1 negativity out of 100 infected

erythrocytes. Parasites (iRBCs) exhibiting the density-dependent death phenotype ("Death") were assessed by brightfield microscopy. Significance was determined by two-way ANOVA with Tukey's post-hoc test for non-confounding interaction effects. HD45-HD50, $p < 1e10^{-7}$; LD45-LD50, $p = 1$; HD50-LD50, $p < 1e10^{-7}$; HD45-LD45, $p = 1$. Mean ± SEM. n = 3.

Figure 3. Failure of parasite growth, schizont maturation and merogony in high-density parasite cultures. Parasites prepared for high and low-density culture as described were live-stained for volumetric analysis using the lipid dye BODIPY-ceramide TR (TRITC) and nucleic acid dye Hoechst 33342 (DAPI). Representative images at 30 and 50hpi indicate inhibition of growth and nuclear division in late stage, high-density parasites (HD) only, compared with normal increases in parasite cell volume and merogony between 30 and 50hpi in low-density parasites (LD). Scale bar, 5µm.

Figure 4. High density conditioned medium inhibits normal parasite development and is stage- and density-specific. (A) Conditioned medium (CM) operates in parasite density ranges relevant to human malaria. Parasites exhibiting the density-dependent death phenotype ("Death") are shown as a proportion of 100 iRBC after treatment with CM harvested from late trophozoites at concentrations of 10^2, 10^3, 10^4 and 10^5 parasites/µl. Percentages are averaged over replicates (n = 3). (B) Schematic of CM harvest and testing. High and low-density parasites are prepared as in Figure 2A and fed fresh media at late ring stage. CM from iRBC and uninfected erythrocytes are harvested by pelleting cultures and removing supernatant after 18 hours of incubation. CM is tested by adding to low-density, late stage trophozoites (~30hpi) and assessing for changes in morphology and replication rate after 12 hours and 24 hours, respectively. (C) CM harvested from low parasite density (LD) cultures and uninfected erythrocytes (U) does not inhibit normal development, compared to CM harvested from high parasite density (HD) cultures. n = 3. Differential counts are given as percent of 100 iRBC. R: rings; T: trophozoites; S: schizonts; Ab: aberrant parasites that exhibited the density-dependent death phenotype during late stage development. (D) CM was harvested from high-density parasite cultures at varying stages and assessed for stage-specific killing activity on low-density cultures during maturation. ER: bursting schizont to early ring, 0-8hpi; LR: late ring, 8-16hpi; ET: early trophozoite, 18-30hpi; T/ES: trophozoite and early schizont, 18-36hpi; Ctrl: fresh complete culture media. n = 3. (E)

Titration of HDCM in complete culture medium below 80% abrogates killing activity. n = 6. (F) CM harvested from 3D7 HD cultures exhibits inter-isolate activity when incubated on cultures of *P. falciparum* isolates Dd2, HB3, D6, and 1776. Ring stage parasite density after 24h incubation was used to measure efficacy of killing activity. Mean ± SEM. n = 3.

Figure 5. Essential nutrient concentrations in HDCM. Glucose (left panel) and lactate (right panel) levels were measured in CMs collected in 6-h intervals from high and low parasite density cultures and two uninfected erythrocyte controls over the course of 30 hours. Incubations for infected erythrocytes were initiated using 18hpi parasites. HD: high density; LD: low density; U: uninfected, 5% hematocrit; R: uninfected, 40% hematocrit. Dashed lines indicate threshold concentrations required for parasite viability as described by Jensen *et al*, 1983 [37]. n = 3.

Figure 6. Nutrient replenishment of high-density parasite cultures or HDCM does not prevent density-dependent death. (A) Parasite viability as assessed by ring stage parasite density in low-density test cultures after 24h incubation in complete culture media with titrated levels of glucose. 0-11: mM concentration of glucose added to glucose-free RPMI prior to culture media formulation; Ctrl: complete culture medium; HD: high-density CM; HDG: high-density CM supplemented with 10mM glucose. (B) The effect of glucose supplementation on late stage development of high and low-density cultures was assessed by nuclear staining of cultures at the nominal schizont stage. G-: no added glucose; G+: parasite culture supplemented with an additional 20mM glucose (total of 30mM in fresh culture medium fed at late ring stage); HD, LD: high or low-density parasite cultures. Mean fluorescence intensity (MFI) was determined for parasites stained with SYTO61 to measure nuclear content. Significance was determined by Student's t-test: HD G+ vs. HD G-, $p = 0.004$; LD G+ vs. LD G-, $p = 0.39$. (C) HDCM and LDCM was supplemented with 10mM glucose (G10), 20mM glucose (G20), 20mM lactate (L20), or 40mM lactate (L40), and tested on low-density late stage trophozoites. Ctrl: no supplementation. Left panel: replication rate of test cultures after 24h incubation; right panel: percent density-dependent death ("Death") in test cultures after 12h incubation. (D) HD parasite cultures are rescued by dilution to low density, but not by media replenishment. HD and LD cultures were replenished with fresh complete culture media at 1 or 2 time points as indicated: 30hpi (Δ30), 24hpi and 36hpi (Δ24/36), 30hpi and 36hpi (Δ30/36), or 36hpi and 42hpi (Δ36/42).

HD parasites were diluted 1:6 in fresh complete culture media at 30hpi (Sub30) or 42hpi (Sub42), keeping hematocrit constant. Left panel: replication rate of parasite cultures after 1 cycle of replication; right panel: percent density-dependent death ("Death") in parasite cultures at nominal schizont stage. Ctrl: no media change or subculture. LD controls for Sub-30 or Sub-42 were not diluted but maintained at $5x10^3$ parasites/µl. Starting cultures were initiated at $3x10^4$ parasites/µl (HD) or $5x10^3$ parasites/µl (LD). Mean ± SEM. n = 3 for all assays.

Figure 7. Parasites exposed to high-density vs. low-density conditions exhibit differential gene expression. (A) Functional categorization of differentially expressed genes after treatment of parasites with HDCM compared to LDCM. Transcripts were considered to be differentially expressed where fold change is greater than or equal to 2 and adjusted p-value < 0.05. Functional categorization of differentially expressed genes was determined by gene ontology. (B) Real time PCR of 15 genes confirms microarray expression patterns when comparing between HDCM and LDCM treatment. All genes exhibited significant differential expression after RT-PCR (Student's t-test, $p < 0.05$). All genes except MCA2 showed significant differential expression in the microarray. PFIDs and primers sequences are contained in the supplemental material (Table S11). (C) Barcode plots illustrate distribution of genes in highly differential gene sets as determined by correlation adjusted mean rank test (CAMERA): GO_0020033: antigenic variation, GO_0020025: cytoadherence to microvasculature mediated by parasite protein, GO_0005783: endoplasmic reticulum, and GO_0008654: phospholipid biosynthesis. Enrichment plots above barcode plots show relative enrichment between high and low-density conditions using t-statistics for each gene set. No significant enrichment was observed for the set of dysregulated genes associated with glucose deprivation. Results shown are averaged over replicates (n = 3).

Figure 8. Real time PCR of 44 genes using conditioned medium supplemented with replenished nutrients (HDCM+) or with metabolic by-products (LDCM+). Fold change (log2) represents the ratio of expression values for HDCM+ over LDCM+ and are plotted against -log10 p-value. Blue data points highlight HDCM+/LDCM+ RT-PCR expression values concordant with the microarray expression values for HDCM/LDCM. P-value is determined by Student's t-test, dashed line indicates p = 0.05. Results shown are averaged over replicates (n = 3).

Figure 9. Exposure to high parasite density induces dysregulation of sexual stage transcripts in asexual parasites. (A) Exposure to HDCM induces changes in gametocyte gene RNA transcript levels within 2 hours as compared to parasites exposed to LDCM or UCM. A gametocyte gene set was compiled using 532 genes either coding for known gametocyte markers or whose expression correlated with gametocytogenesis based on published literature. Heat maps indicate dysregulation of gametocyte-associated genes when comparing treatment with HDCM to LDCM or to UCM, but no significant differential expression when comparing treatments between LDCM and UCM. Columns indicate independent biological replicates; rows represent individual genes. Z-scores indicate standard deviations from the mean, centered and normalized for each row giving relative signal intensity between sample columns. Red: upregulated, blue: downregulated. (B) Differential expression of a panel of 39 sexual development markers. Left panel: A panel of 39 gametocyte markers with known roles in gametocytogenesis were arrayed from earliest to latest expression throughout sexual development (rows). Expression values from previously published time course data were clustered using pairwise average linkage (columns). Right panel: Heat map generated for stage-specific gametocyte marker panel using expression data from high and low density CM-treated parasites. Gametocyte marker expression is upregulated in HD samples throughout all stages of sexual development. C. Transcriptional profiles for parasites exposed to HDCM, LDCM, and UCM were correlated with known transcriptional profiles for all stages during the *P. falciparum* lifecycle [49]. Biological replicates were correlated within experimental condition groups to assess extent of biological variation and found to exhibit low variation ($r > 0.98$, all conditions). For all samples, transcriptomes correlated most strongly with late trophozoites, but not with early gametocytes. All Pearson correlation coefficients are significant ($p < 0.0001$). U1-3; LD1-3; HD1-3: biological replicates for trophozoites treated with UCM, LDCM, and HDCM, respectively. Mz: merozoite; ER: early ring; LR: late ring; ET: early trophozoite; LT: late trophozoite; ES: early schizont; LS: late schizont; G1-12: gametocyte commitment to maturation; Spz: sporozoite.

Table 1. High parasite density environment induces global changes in gene expression

Table 1. (A) Global changes in gene expression are induced by a 2-hour incubation in HDCM when compared with gene expression in LDCM ($n = 3$). Number of genes with statistically significant differential expression is indicated. (B) Dysregulation of the gametocyte-associated

gene set. Early, peak expression during gametocyte developmental stages I/IIA; Middle, stages IIB/III; Late, stages IV/V. Numbers of genes with statistically significant differential expression and at least 1.5x fold change are indicated. (C) Dysregulation of *P. falciparum* pathways under high-density conditions measured by rotation gene set testing (ROAST). Differential expression of gene sets associated with sexual development, cell death mechanisms, epigenetic modifications or variant gene families, including gene set size and directionality of expression in high density conditions (up, down or bidirectional). Up/Down: total number of significant genes up- or down-regulated per gene set. Overall gene set significance is indicated by false discovery rate < 0.05 (FDR). PFIDs for gene sets are contained in the supplemental material (Table S6). Data for variant expressed genes, H3K9me3-enriched genes, and HP1-enriched genes are found in [45–48].

Table 1. High parasite density environment induces global changes in gene expression

A. Global gene expression	**Total**	**Upregulated**	**Downregulated**
Genes on chip	4298		
Differentially expressed genes, all significant	1384	593	791
- Two fold or greater change	666	203	463
- Less than two fold change	718	390	328
B. Sexual development genes	**Total**	**Upregulated**	**Downregulated**
Differentially expressed genes, all significant	123	72	51
- Early (Stages I-II)	51	31	20
- Middle (Stages II-III)	49	31	18
- Late (Stages IV-V)	23	10	13

C. Gene set dysregulation	Size (Up/Down)	Direction	FDR
Gametocyte-associated genes, full panel	711 (90/61)	Up	4.92×10^{-2}
Gametocyte genes, verified (36)	36 (6/2)	Up	3.11×10^{-3}
Apoptosis	25 (6/5)	Bidirectional	1.35×10^{-6}
Glycolysis	23 (2/7)	Down	1.19×10^{-3}
Autophagy	6 (0/3)	Down	5.25×10^{-6}
Kinase	130 (22/21)	Bidirectional	4.15×10^{-9}
Mitochondrial antioxidant system	10 (0/3)	Down	2.46×10^{-3}
Thioredoxin/glutaredoxin/peroxiredoxin	16 (0/4)	Down	8.24×10^{-4}
Variant expressed genes, 3D7	138 (18/2)	Up	4.15×10^{-4}
H3K9me3-enriched genes	384 (19/1)	Up	1.52×10^{-3}
HP1-enriched genes	425 (36/3)	Up	2.11×10^{-3}

Table 2. Density-induced alterations in *P. falciparum* functional pathways

Table 2. Enrichment of *P. falciparum* pathways in parasites cultured under high and low parasite density conditions, as determined by competitive gene set testing using correlation adjusted mean rank test (CAMERA) and averaged over replicates (n = 3). For each category, the number of dysregulated pathways is indicated. "Enrichment profile" indicates whether functional pathways are upregulated in the high-density condition compared to low density ("High") or in the low-density condition compared to high density ("Low"). Significance of gene set enrichment was determined by false-discovery rate q-value < 0.05.

Table 2. Density-induced alterations in *P. falciparum* functional pathways

Category	No. of Pathways	Enrichment Profile	
		High	Low
Antigenic variation and cell adhesion	14	x	
Apicoplast	2		x
Endoplasmic reticulum / protein transport	6		x

Export	1		x
Metabolism	2		x
Motor activity and cytoskeletal rearrangements	5	x	
Nuclear component	2	x	
Ribosome biogenesis	2	x	

1353

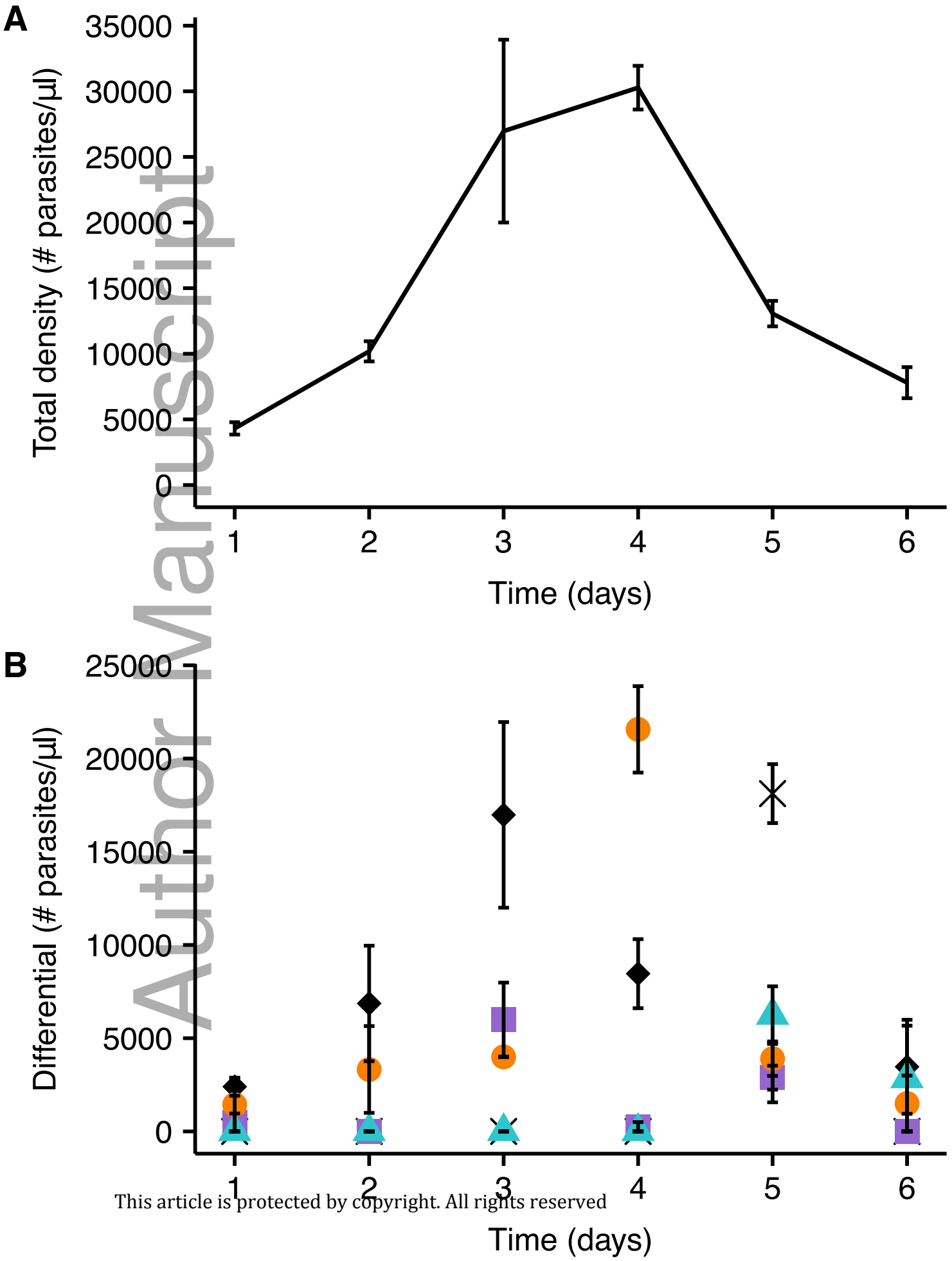

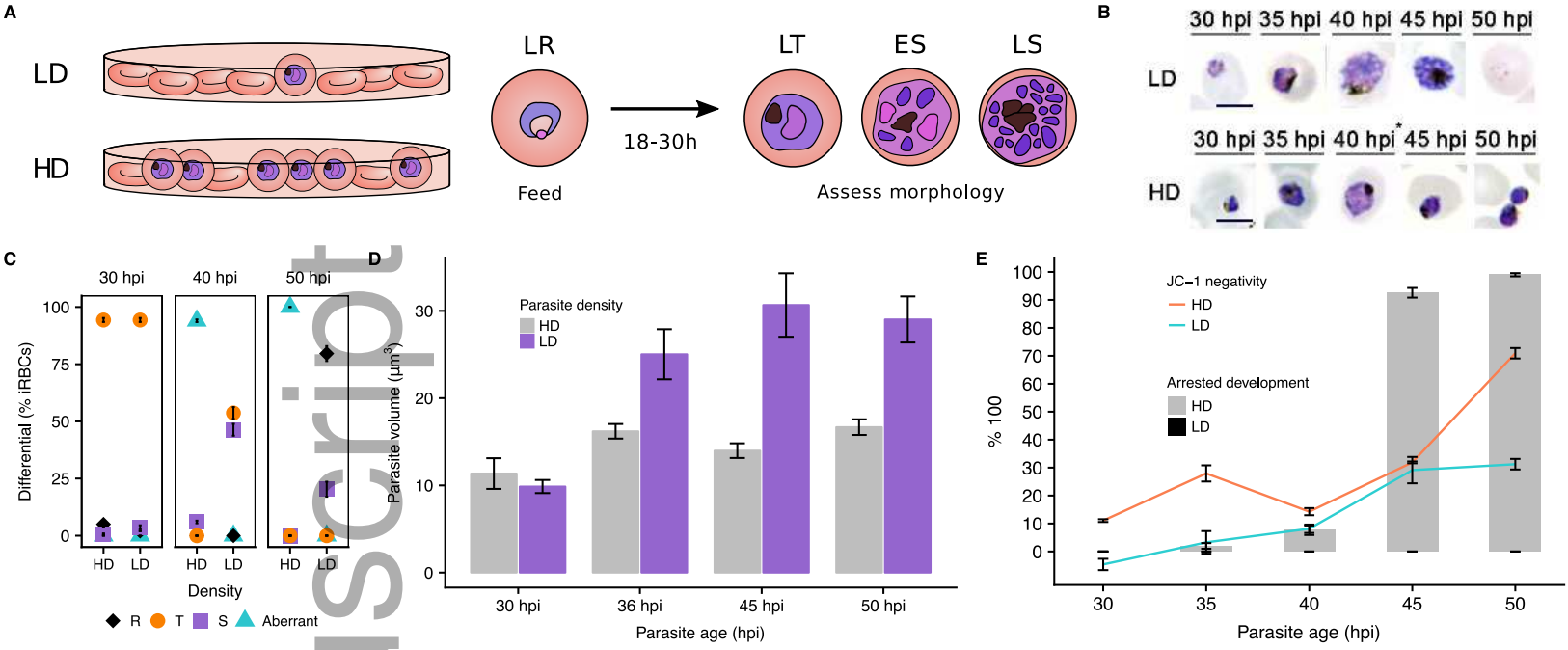

febs_14370_f2.eps

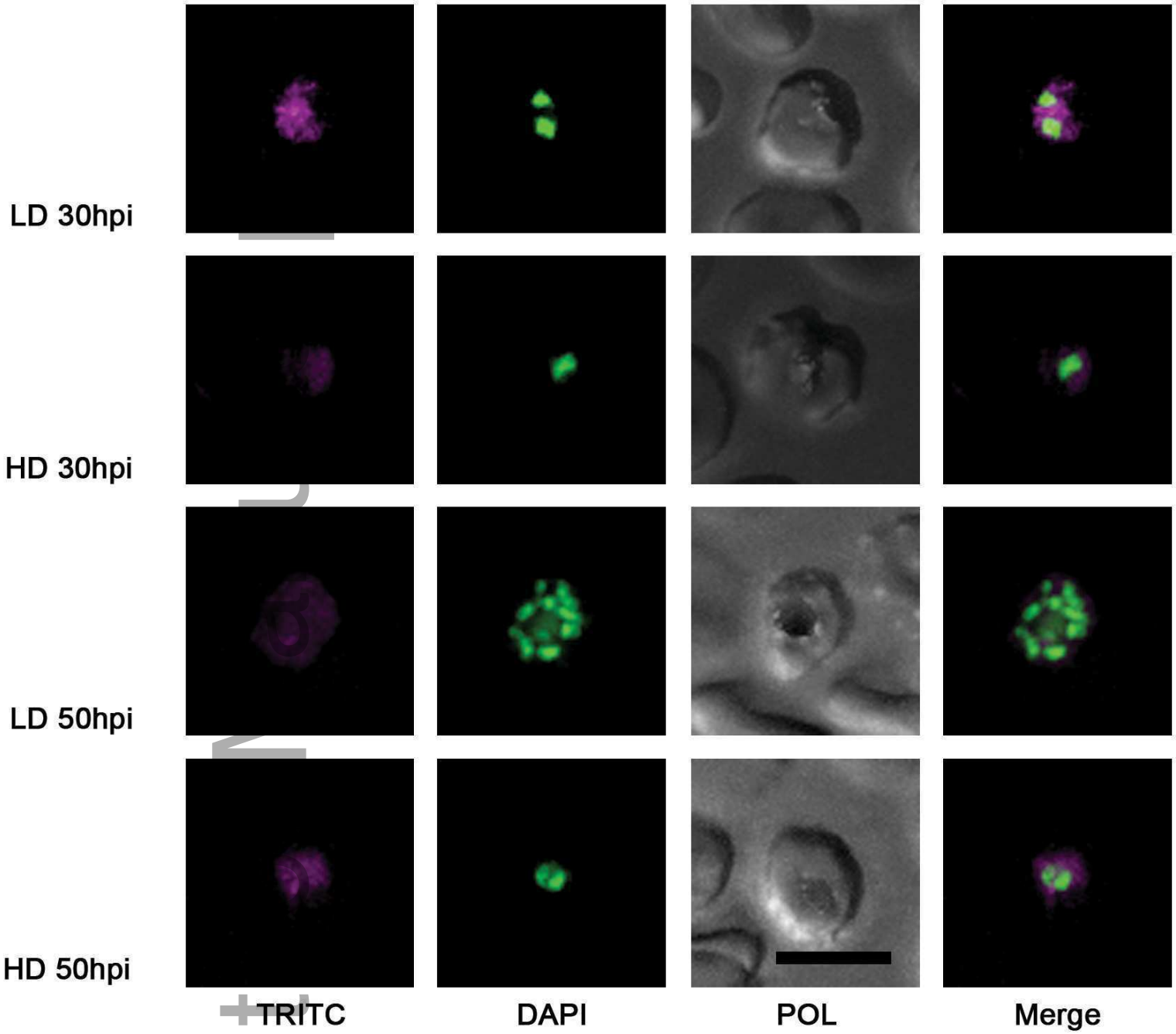

febs_14370_f3.eps

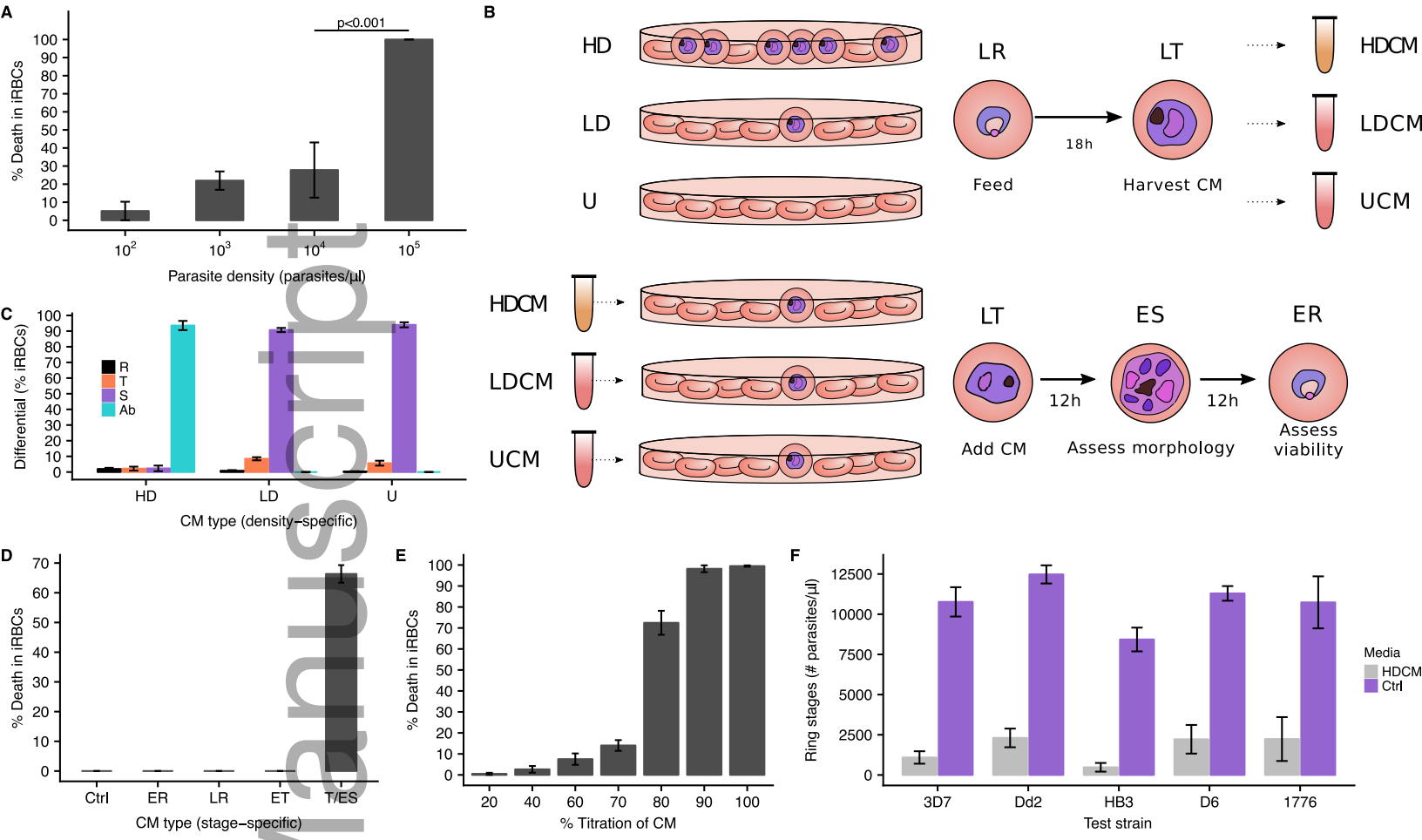

febs_14370_f4.eps

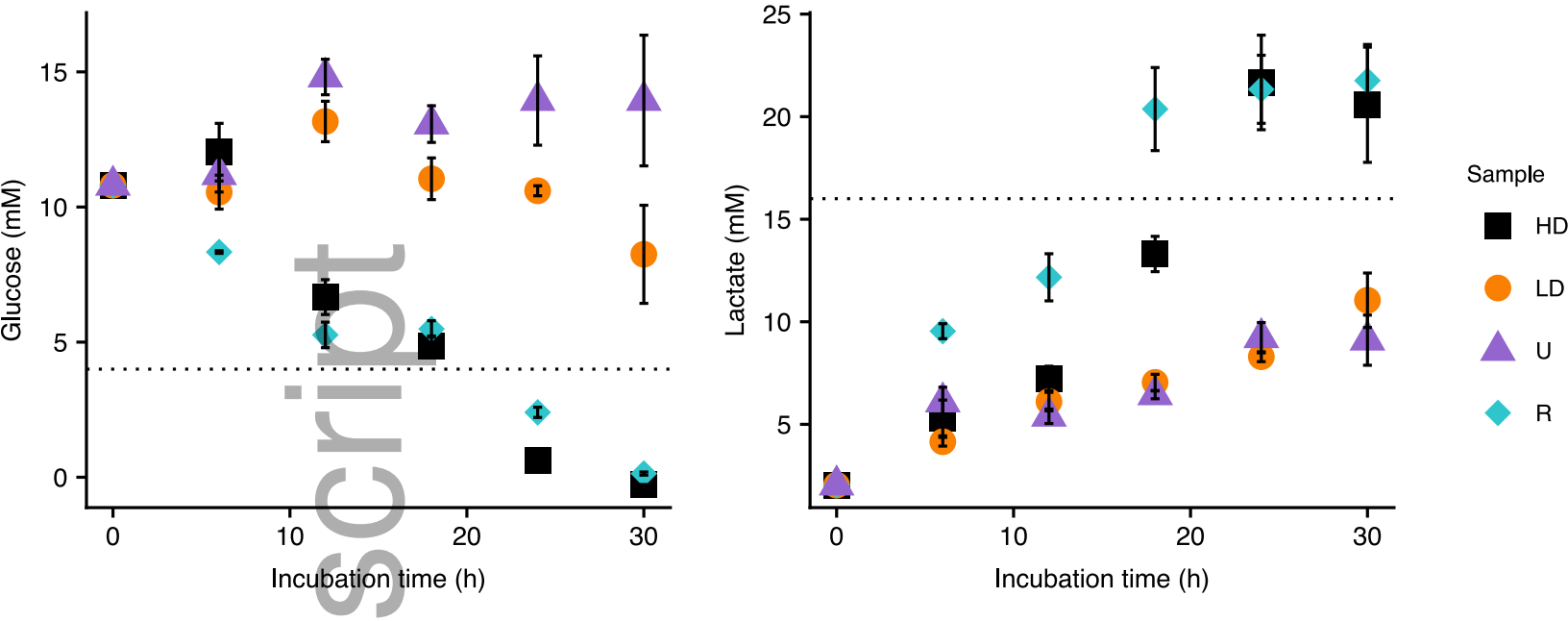

febs_14370_f5.eps

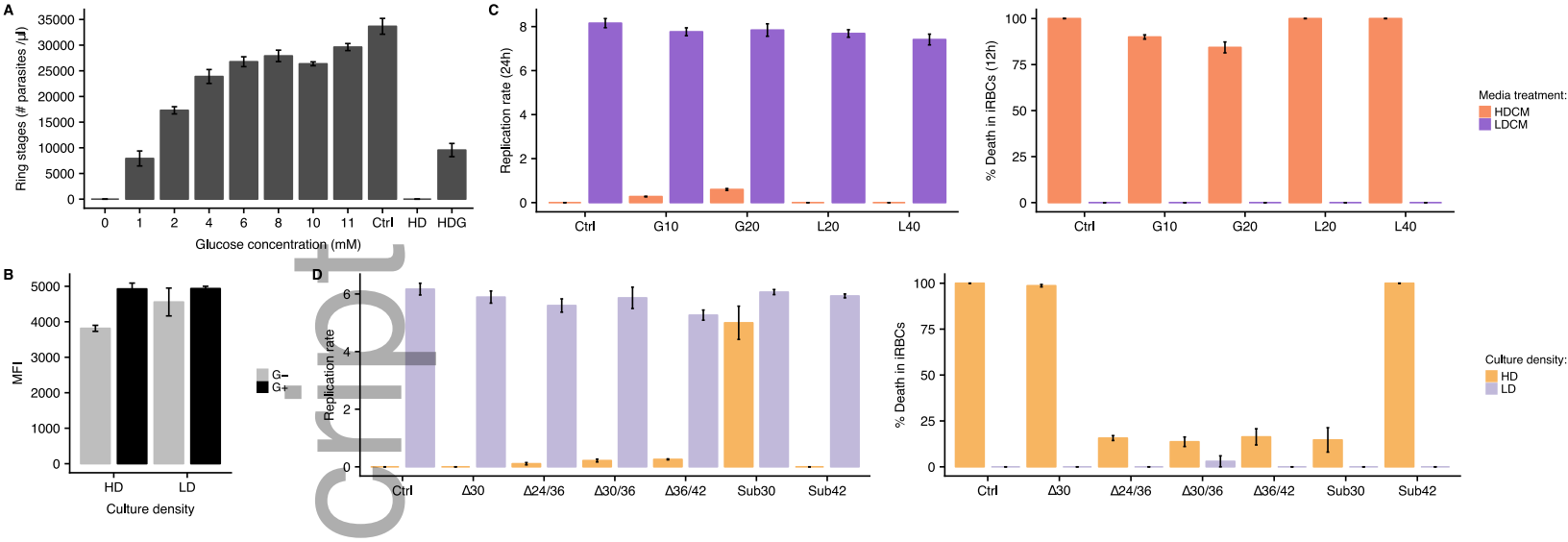

febs_14370_f6.eps

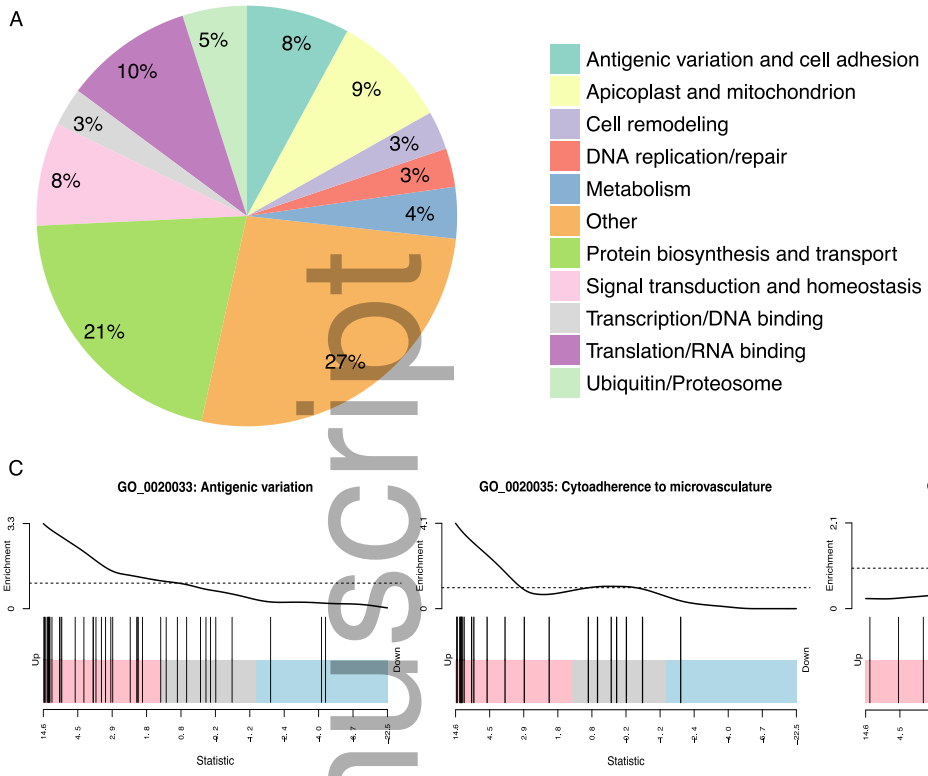

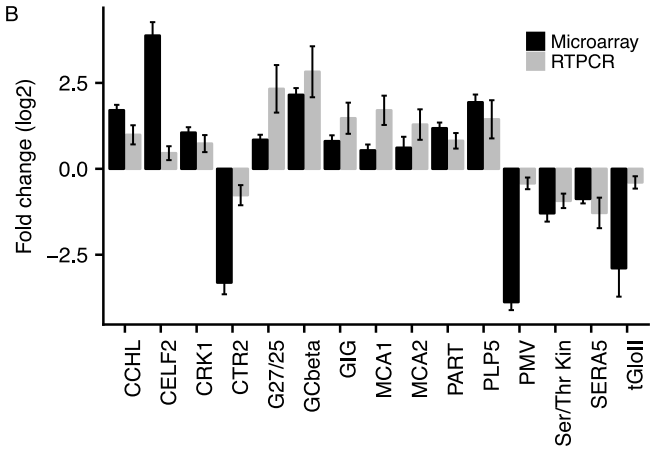

febs_14370_f7.eps

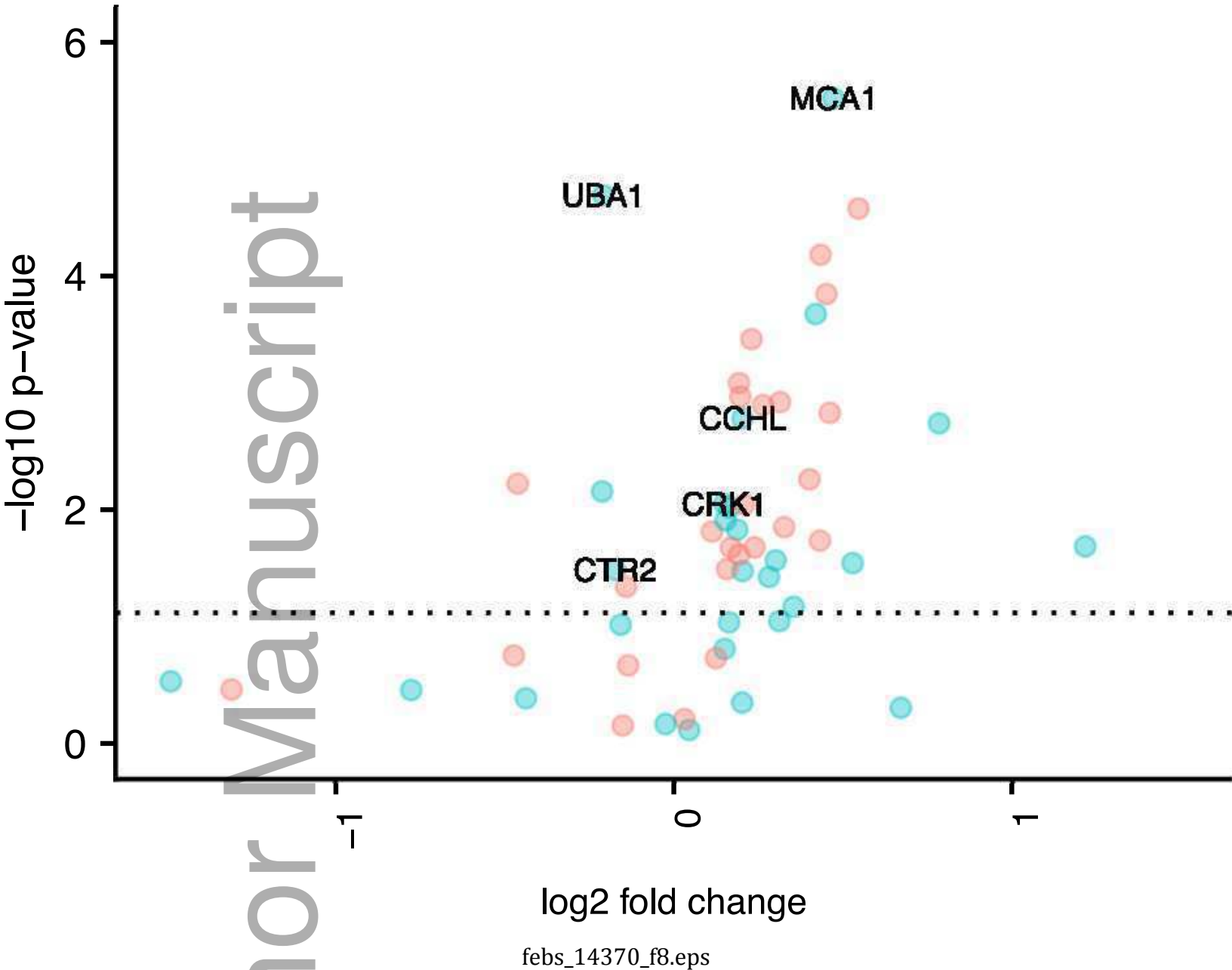

febs_14370_f8.eps

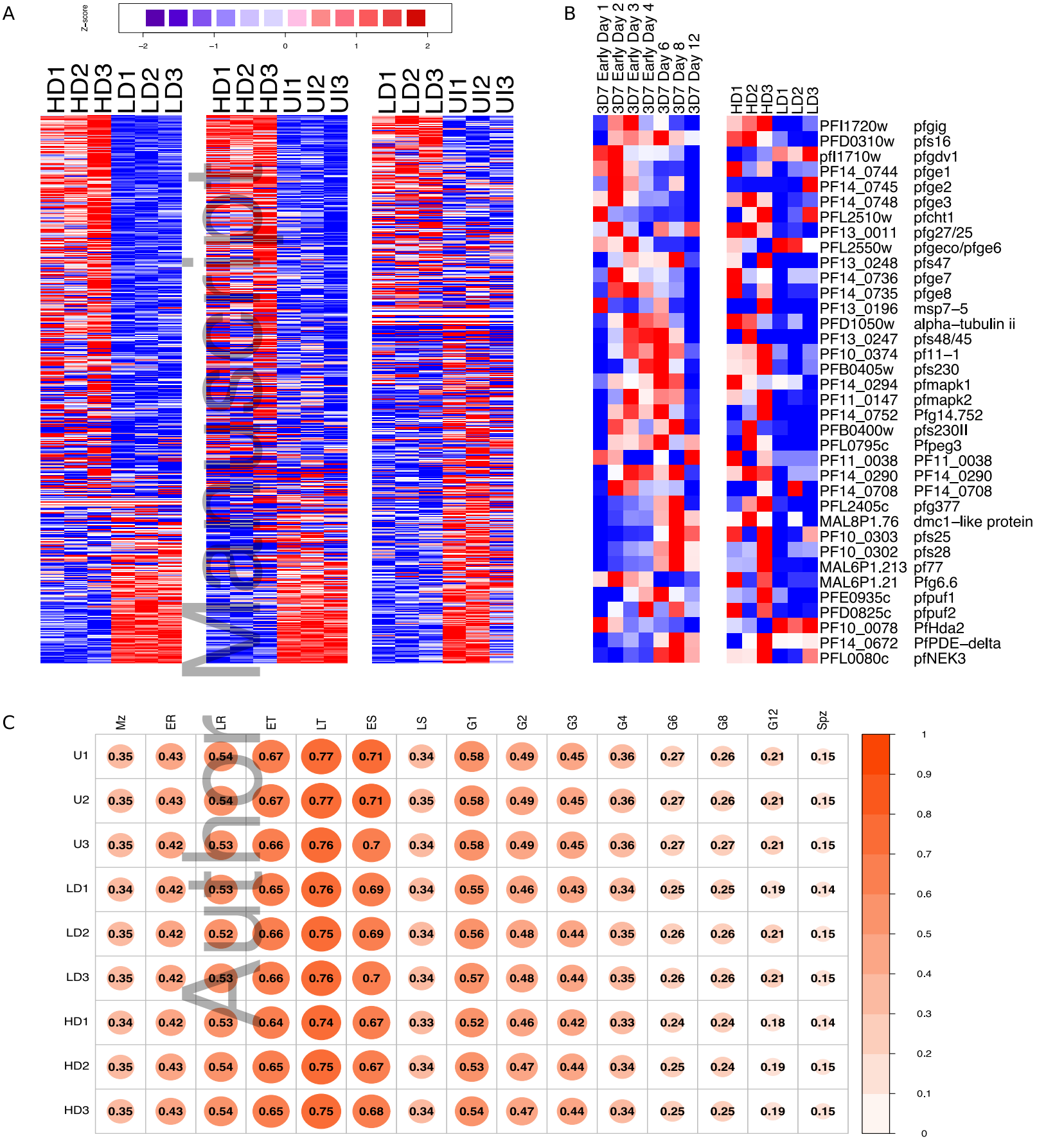

febs_14370_f9.eps